TECHNICAL UNIVERSITY OF LIBEREC

FACULTY OF TEXTILE ENGINEERING

DIPLOMA THESIS

2011 **Nhlanhla Cyril Kumalo**

Technical University of Liberec

Faculty of Textile Engineering

Department of Textile Technology

Textile Chemical Technology

Photocatalysis application in wastewater treatment processes

Supervisor : Eng. B.Sc. Jarmila Studničková, PhD.

Consultant : Assoc. Prof. Eng. Jakub Wiener, PhD.

Number of text pages: 78

Number of figures 28

Number of tables 14

Number of references 35

STATEMENT

I was informed about the copyright of my diploma thesis which relates to the law number 121/2000, especially section 60 – school publication.

I acknowledge that Technical University of Liberec (TUL) does not breach my copyright when using my thesis for internal purposes of TUL.

Shall I use my thesis or its license utilisation; I am obliged to inform TUL in advance. This way, TUL has the right to claim the expenses for realisation of my work to full extent.

I elaborated my thesis independently using mentioned resources and on the basis of an advice given by the supervisor and consultant.

In Liberec

Nhlanhla Cyril Kumalo Date

ACKNOWLEDGEMENTS

First and foremost, I would like to express my deepest gratitude to my supervisor Eng. B.Sc. Jarmila Studničková, PhD and consultant Assoc. Prof. Eng. Jakub Wiener, PhD for their endless support, patience, supervision and encouragement during this study and all the time. I could never complete this work without her vision and support.

I would like to express my thanks to Van Dyck Carpets Company with their supportive and motivated team mates. Many thanks to my sister – Buyisiwe Khumalo and my two brothers Nkosinathi and Senzo Khumalo. I dedicate this work in loving memory of my mother and father who passed away a decade ago - were not near me but you were always with me. Without your encouragement I could never have completed this work. I love you. Finally I would like to express my warmest thanks to Nasirah Govindsamy for her endless support and encouragement. I wish to live with you forever…

Thanks to DED (Department of Economic Development) for their financial support.

ABSTRACT

Ten textile dyes (azo-dyes (CI Disperse Red 50, CI Direct Yellow 44, CI Reactive Blue 19, CI Reactive Blue 4, 1:1 metal complex CI Acid Blue 158, 1:2 metal complex CI Acid Red 213 and CI Acid Yellow 11), anthraquinone dyes (CI Disperse Red 121), oxazine dyes (CI Direct Blue 106) and nitro dyes (CI Disperse Yellow 42). were photocatalytically treated for colour removal in TiO2 suspension. Their decolouration rates were compared to the standardised methods; flocculation and coagulation. It was demonstrated the azo dye (CI Acid Red 213) and oxazine dye (CI Direct Blue 106) were highly degraded by photocatalysis with decolourization of 50 % after 15 min and 30 min and 84 % after 60 min with azo dye (CI Acid Yellow) being not degraded – from 5 – 30 min was 50 % darker and gradually back to the original (standard 100%) colour in 40 – 60 min. Disperse dyes on photocatalytic degradation gained more weight becoming darker after 30 min, which could be due photocatalytic degradation of auxiliary (dispersing agents) agents. The results indicate that photocatalytic colour degradation on CI Acid Red 213 and CI Direct Blue 106 was faster than on standardised methods.

Key words - photocatalysis, titanium oxide P25 Degussa, UV light

LIST OF FIGURES

LIST OF TABLES

LIST OF ABBREVIATONS

CB	Conduction Band
VB	Valence Band
AOPs	Advanced Oxidation Processes
UV	Ultraviolet Light
VIS	Visible Light
TiO_2	Titanium Dioxide
PES	Polyester
CO	Cotton
WO	Wool
PA	Polyamide
PAN	Polyacrylonitrile
TOC	Total Organic Compounds
DOC	Dissolved Organic Compounds
TEM	Transition Electron Microscope
$Ca(OH)_2$	Calcium Hydroxide
L – H	Langmuir–Hinshelwood
eV	Electron Volt
e^-	Excited Electron
h^+	Positive Hole

Table of contents

1. INTRODUCTION

The use of conventional textile wastewater treatment processes becomes drastically challenged to environmental engineers with increasing more and more restrictive effluent quality by water authorities. Conventional treatment such as biological treatment discharges will no longer be tolerated as 53% of 87 colours are identified as non-biodegradable.

Textile dyes and other industrial dyestuffs constitute one of the largest groups of organic compounds that represent an increasing environmental danger. About 1–20% of the total world production of dyes is lost during the dyeing process and is released in the textile effluents. The release of those colored waste waters in the environment is a considerable source of non-aesthetic pollution and eutrophication and can originate dangerous by-products through oxidation, hydrolysis, or other chemical reactions taking place in the wastewater phase [17]

Decolourization of dye effluents has therefore received increasing attention. For the removal of dye pollutants, traditional physical techniques (adsorption on activated carbon, ultrafiltration, reverse osmosis, coagulation by chemical agents, ion exchange on synthetic adsorbent resins, etc.) can generally be used efficiently. Nevertheless, they are non-destructive, since they just transfer organic compounds from water to another phase, thus causing secondary pollution. Consequently, regeneration of the adsorbent materials and post-treatment of solid-wastes, which are expensive operations, are needed. Due to the large degree of aromatics present in dye molecules and the stability of modern dyes, conventional biological treatment methods are ineffective for decolourization and degradation. Furthermore, the majority of dyes is only adsorbed on the sludge and is not degraded [17, 22]. Chlorination and ozonation are also being used for the removal of certain dyes but at slower rates as they have often high operating costs and limited effect on carbon content. These are the reasons why advanced oxidation processes (AOPs) have been growing during the last decade since they are able to deal with the problem of dye destruction in aqueous systems. AOPs were based on the generation of very reactive species such as hydroxy radicals ($^{\bullet}OH$) that is a strong oxidizing (E_0 = 2.8 V) agent capable of mineralizing most organic pollutants. AOPs such as Fenton and photo-Fenton catalytic reactions, H_2O_2/UV processes and TiO_2 mediated photo-catalysis have been studied under a broad range of experimental conditions in order to reduce the colour and organic load of dye containing effluent waste waters [17].

Photocatalysis using TiO_2 (P25 Degussa) as photo-catalyst appears as the most emerging destructive technology. The key advantage is its inherent destructive nature: it does not involve mass transfer; it can be carried out under ambient conditions (atmospheric oxygen is used as oxidant) and may lead to complete mineralization of organic carbon into CO_2 and H_2O. Moreover, TiO_2 photocatalyst is largely available, inexpensive, non-toxic and show relatively high chemical stability. The utilization of combined photocatalysis and solar technologies may be developed to a useful process for the reduction of water pollution by dying compounds because of the mild conditions required and their efficiency in the mineralization [17].

In the present work, the colour removal on wastewater using photocatalysis was compared to standard methods (flocculation and coagulation). The dyes treated are the azo-dyes (Disperse Red 50,Direct Yellow 44, Reactive Blue 19, Reactive Blue 4, 1:1 metal complex Acid Blue 158, 1:2 metal complex Acid Red 213 and Acid Yellow 11), anthraquinone dyes (Disperse Red 121), oxazine dyes (Direct Blue 106) and nitro dyes (Disperse Yellow 42).

2. LITERETURE REVIEW

2.1 WATER IN TEXTILES

The textile industry is very water intensive. Water is used for cleaning the raw material and for many flushing steps during the whole production. Produced waste water has to be cleaned from, fat, oil, colour and other chemicals, which are used during the several production steps. The cleaning process depends on the kind of wastewater (not every plant applies the same production process) and also on the amount of used water. Also not all plants use the same chemicals, especially companies with a special standard (environmental) try to keep water cleaned in all steps of production. So the concepts, to treat the water can differ from each other.

It is quite difficult to define a general quality standard for textile water reuse because of the different requirements of each fibre (silk, cotton, polyester etc.), of the textile process (e.g., scouring, desizing, dyeing, washing, etc.) and because of the different quality for final product.

The textile dyeing and finishing sector uses large volumes of water and substantial quantities of complex chemicals. Companies operating in this sector are facing significant challenges, many associated with the acquisition and disposal of these essential raw materials. In particular, the charges incurred for mains water supply and effluent disposal are increasing, and companies need to address these issues to save money and remain competitive

Wet processes in the textile industries require water of very good quality concerning mainly content of dyes, detergents, and suspended solids. Therefore, a purification treatment to recycle water must have much better performances than for simple discharge according to the limits imposed by legislation. In order to meet legislative requirements, textile waste waters are usually treated in a chemical-physical or most commonly in an active sludge biochemical plant. Instead, in order to have water that can be recycled in production cycles (especially dyeing processes) water needs further treatments to be re-used. Among all the possible purification systems that were proposed for textile wastewaters, oxidative treatments seem to be promising because they really involve a degradation process of the pollutants contained, although never complete. They are moreover very effective towards the oxidation of chromophoric structures of dyes, removing colour which is the main “disturbing” factor for water recycle in textile industry.

2.2 TEXTILE DYES

Textile dyes are chemical compounds characterised by absorbing light in the visible region of the electromagnetic spectrum (400 – 700 nm) and this is the reason why they are coloured [1]. Most dyes share the same basic chromogenic structure, being differentiated by either physical size of the molecule or by the presence of the solubilising groups, such as sulfonic acid and quaternary ammonium groups. The main chromogens are azos, anthraquinones, indigoids, polymethines (cyanines), nitro (phthalocyanines), oxazines and aryl carboniums [2].

In practice it is reported that more than 90 % of the organic chemicals and auxiliaries used in dyeing processes does not stay on fibre and found in emissions. The fixation rate of individual dye varies according to type of fibre, shade and dyeing parameters. Estimated fixation rates for different types of dyes, processes and fibres are given in Table 2.1. Fixation rates of vat sulphur and disperse are 85 %, 70 % and 95 % which indicate that about 15 %, 30 % and 5 % dyestuff applied remains in wastewater (Table 2.1).

2.2.1 IMPORTANT DYE STRUCTURAL CLASSES

2.2.1.1 Azo Dyes

Azo dyes make up to 60 – 70 % followed by anthraquinones 15 % (most commercially important group of dyestuffs, manufactured on a very large scale and used in most application areas) of all textile dyestuffs and are not removed from textile wastewater via conventional biological treatments. It has been reported that some of them are toxic, mutagenic, and carcinogenic compounds. Their resistance to biological and even chemical degradation makes them hazardous for the environment even at low concentration. They represent about 50% of the worldwide production and correspond to an important source of contamination considering that approximately 15% of the synthetic textile dyes are lost in waste streams during manufacturing or processing operations [22].

They are characterised by one or more chromic –N=N- groups, as indicated in Figure 2.1 [1, 2]. Azo dyes found in different categories, i.e. acid, basic, direct, disperse and reactive. The amount of dye that does not bind to the fibre and is lost to wastewater is during textile processing is estimated from 5 – 10 % to 50 % in the case of reactive dyes, and the azo dye concentration in wastewater produced by textile industries varies from 5 – 1,500 mg/l [4].

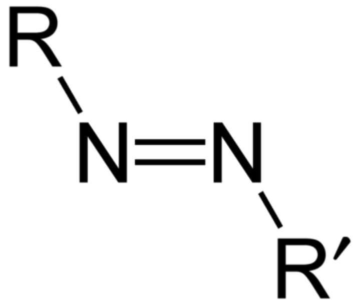

Figure 2.1 General chemical formula of azo compounds.

Toxicity of Azo dyes

It is known that certain amines used to manufacture azo dyes and any synthetic dyestuff caused bladder cancer, especially 2-naphthylamine, benzidine and 4 aminodiphenyl. Upon this it was noted that the list of potentially carcinogenic amines is much longer and could be actually generated by metabolic reductive cleavage of these dyes that are made using these amines as their diazo components. Azo dyes are xenobiotic strongly resistant to biological degradation processes: they are not degraded in conventional aerobic sewage treatment plants and became a great environmental hazard.

Azo dyes released in the environment are an important risk for human health, as a potential source of carcinogenic aromatic amines. Azo dyes can enter the human body through the food chain or by skin contact; in the liver and in the gastrointestinal tract, they are reduced by azoreductases to aromatic amines, which induce urinary bladder cancer in humans and tumours in experimental animals.

Therefore, to avoid the risk for human health due to azo dyes, their complete degradation is of main importance: decolourization, which is simple done by flocculation and coagulation, is not sufficient, if their metabolites are not completely mineralized.

Table 2.1 Estimated fixation rate for different types of dyes, processes and fibres [3]

Type of Dye	Process	Type of Fibre	Average Fixation Rate	Range [%]
Disperse	C	CE, PES	95	88 -99
Disperse	P		97	91 -99
Disperse	B	PES	97	95 - 99
Direct	B	CO	88	64 - 96
Reactive	B	WO	95	90 -97
Reactive	B	CO	75	65 - 90
Reactive	C	CO	80	70 - 95
Vat	P	CO	75	60 - 90
Vat	C		85	80 - 95
Vat		CO	75	70 - 80
Sulphur	C	CO	90	85 - 95
Sulphur	P		70	60 - 90
Acid, 1 SO^{-3} group	B	PA, PAN	70	65 - 95
Acid, >1 SO^{-3} group	B	CO	90	85 - 93
Basic	B	PAN, PES, PA, CO	95	85 - 98
Azoic (naphthol)	C		99	96 - 100
Azoic (naphthol)	P		87	76 - 89
Metal complex	B		94	80 - 91
Pigment	C		100	
Pigment	P		100	98 - 100

2.2.1.2 Anthraquinone dyes

This is the second most important group in dyestuff chemistry (constitutes about 15% of dye in the textile industry). According to Bamfield P (2001), the main advantage of this group in the dyeing process is their bright red and blue dyes with good fastness properties (washing, rubbing, perspiration and more important light fastness). However they have low tinctorial strength compared to azo dyes, their molar absorption coefficients are less than half those observed with azo dyes of comparable shades. They are characterised by anthraquinone ring system, Figure 2.2 shows the ring system of 9, 10 anthraquinone. The major application groups are vat dyes, disperse dyes and acid dyes [5].

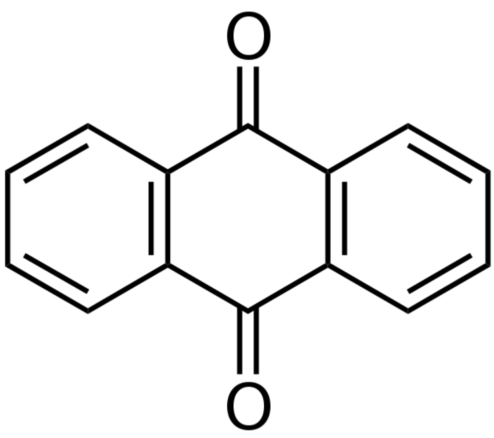

Figure 2.2 General chemical formula of 9, 10 anthraquinone.

2.2.2 Types of dyes

2.2.2.1 Reactive dyes

Reactive are the most important group in dyeing cotton fibres, silk, producing dyed fibres that combine bright shade with excellent fastness properties, especially fastness to washing. Reactive dyeing involves the formation of a covalent bond between the dyestuff and the fibre; specifically by the reaction of functional groups within the dyestuff molecule and the hydroxy groups on the cellulose fibre. Typical structures include the azo (Figure 2.3), anthraquinone, triphenodioxazine or copper phthalocyanine chromophores [2, 8].

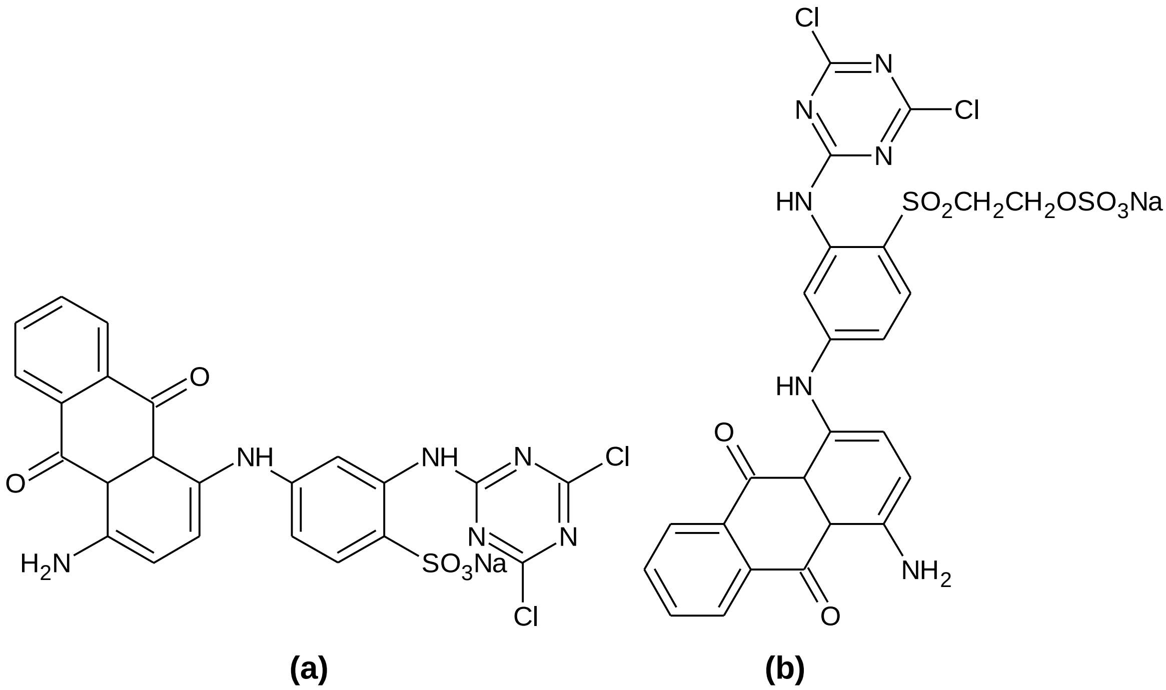

Figure 2.3 CI Reactive Blue 4 (a) and CI Reactive Blue 19 (b)

The main features of reactive dyes are the chromic system, the sulphonate groups for water solubility, the reactive groups, and the bridging groups that attaches the reactive group either directly to the chromophore or to some other parts of the dye molecule.

During dyeing under the alkaline conditions, which is necessary for the dye – fibre reaction (covalent bonding), hydroxide ions also react with the reactive group of the dye in much the same manner as the cellulosate ion resulting in hydrolysed dye that is incapable of reaction with the fibre. After dyeing, any unreacted and hydrolysed dye present in the cotton must be removed by thorough washing to the effluent. This ensures that no colour will bleed from the cotton on subsequent washing during use.

2.2.2.2 Acid dyes

Fibres like nylon, silk and wool because of their common structural features they are dyed using the same dyes (acid dyes); the common structural features are, (1) the amide groups –NHCONH – linking segment of the polymer chains and (2) the amino and carboxylic groups at the end of chains or on side chains for wool. These fibres are also characterised by their ionic nature due to the presence of weakly basic amino groups and weakly acidic carboxylic acid groups thus resulting in the overall charge on fibre becoming positive due to increased acidity of the dyeing bath [2, 6].

Acid dyes are classified according to chemical structure (azo, anthraquinone, xanthene and triphenylmethane chromophores) and dyeing characteristics (depending on the application pH are: level dyeing acid dyes – pH 2.5–3.5, fast acid dyes – pH 3.5–5.0, acid milling dyes – pH 5.0–7.5 and super milling dyes – pH 7.0 The name 'acid dye' derived from the use of an acidic dyebath. According to Colour Index (CI) most pre-metallised and mordant dyes are acid dyes as shown in Figure 2.4 below.

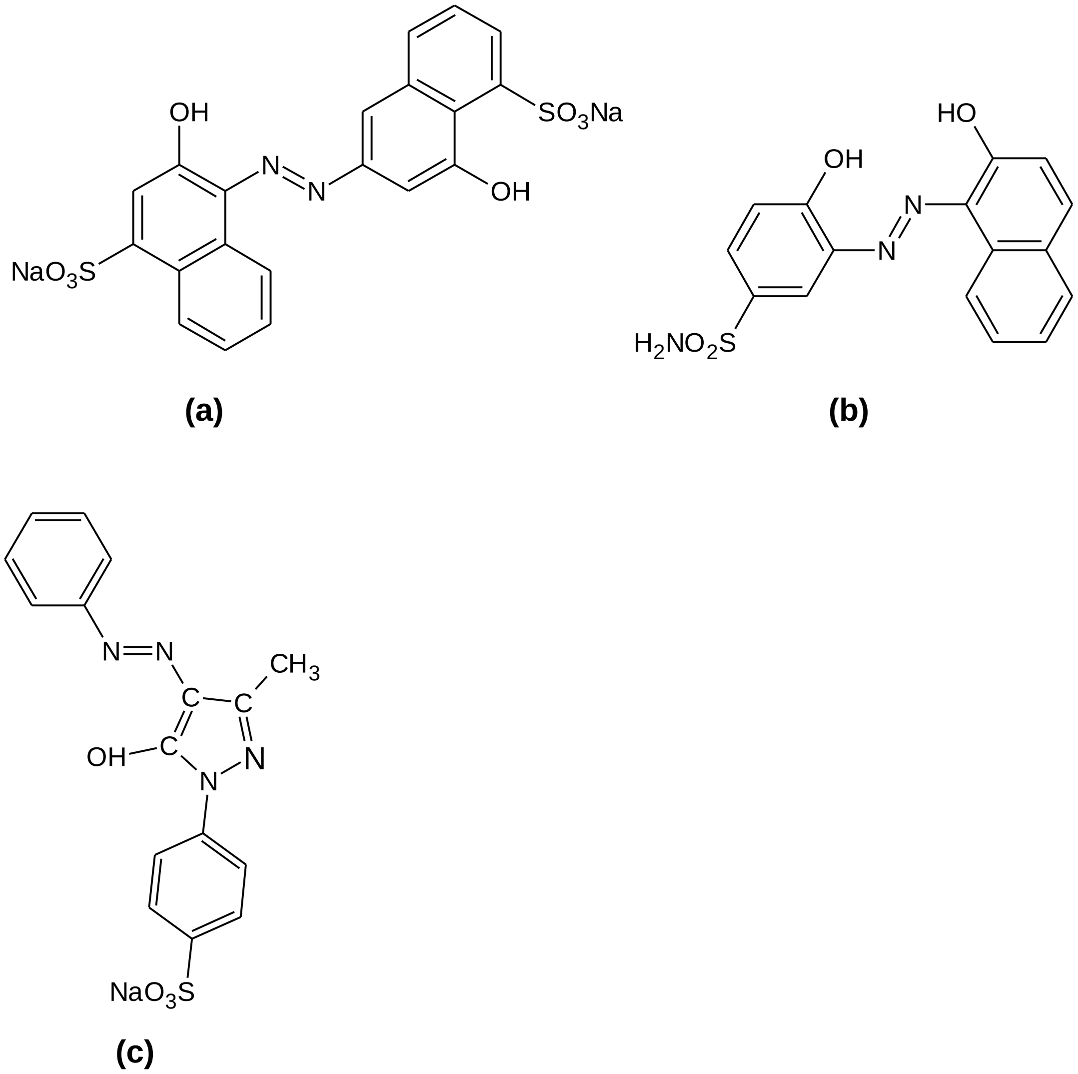

Figure 2.4 (a) CI Acid Blue 158, (b) CI Acid Red 213 and (c) CI Acid Yellow 11

2.2.2.3 Direct dyes

Direct cotton dyes have inherent substantivity for cotton, and for other cellulosic fibres. Their aqueous solutions dye cotton usually in the presence of an electrolyte such as NaCl. Many direct dyes are relatively inexpensive. They are available in a full range of hues but are not noted for their colour brilliance. Their major drawback is their poor to moderate fastness to washing.

Although direct dyes often have similar structures to acid dyes, they generally have higher molecular weights and extended coplanar molecular structures. There is, however, no clear demarcation between acid and direct dyes. Some direct dyes dye protein and nylon fibres just as a few acid dyes will also dye cotton. Many of the older azo direct dyes (Figure 2.5) based on benzidine and its derivatives, such as Congo Red, and some made from 2-naphthylamine, are no longer manufactured in many countries. Benzidine and 2-naphthylamine are proven carcinogens [6].

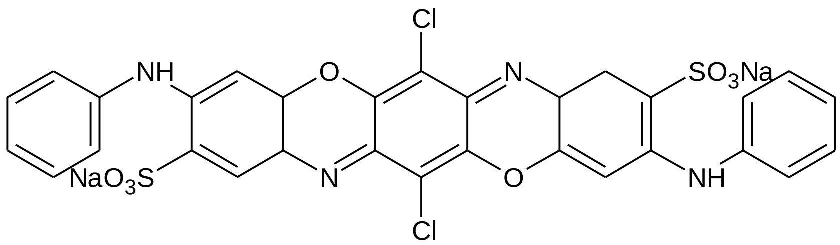

(a)

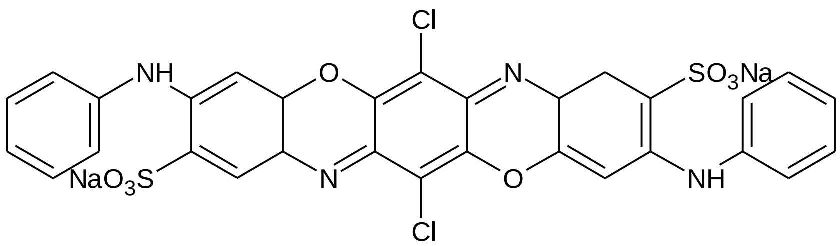

(b)

Figure 2.5 (a) CI Direct Blue 106 and (b) CI Direct Yellow 44

2.2.2.4 Disperse dyes

These non-ionic dyes are relatively insoluble in water at room temperature and have only limited solubility at higher temperatures. They do, however, possess substantivity for hydrophobic fibres such as nylon and polyester, in which they are quite soluble. As their name implies, these dyes are present in the dyebath as a fine aqueous suspension in the presence of a dispersing agent. The water dissolves a small amount of the dye in monomolecular form. The hydrophobic fibres then absorb the dye from the solution. Because these dyes are non-ionic organic compounds of relatively low molecular weight, many sublime on heating and dyeing by absorption of the dye vapour is also possible [6].

There are many thousands of azo disperse dye structures because of the numerous substitution patterns possible in the diverse diazonium ion and coupling components. Colours that are less typical of simple azo compounds, such as greenish-yellow and blue are also possible using more specialised components. These may have heterocyclic units or cyano substituents.

Anthraquinone disperse dyes are usually 1-hydroxy or 1-amino derivatives. These have bright colours ranging from red through to blue. Simple anthraquinone dyes have low molar absorptivities compared to azo compounds and therefore give dyeings of lower colour yield. Apart from a few bright pinks and blues, anthraquinone disperse dyes are gradually being replaced. Structures of anthraquinone, azo and nitro disperse dye structures are shown in Figure 2.6 below.

There are no true green or black disperse dyes. Dyes with both red and blue light absorption bands for greens, or with several overlapping absorption bands for blacks, are difficult to prepare. A major constraint for disperse dye structures is the relatively low molecular weight that the dye must have to be slightly water-soluble and to be able penetrate into hydrophobic synthetic fibres. A combination of blue and yellow dyes gives green dyeings. Blacks require an after treatment of the dyeing involving diazotisation of the absorbed dye containing a free primary amino group followed by reaction with a coupling component. Black disperse dyes may also be mixtures of dull orange, rubine and navy dyes. Many disperse dyes are mixtures generated by the reactions used in their synthesis. Techniques such as thin layer chromatography are useful for establishing the number of components.

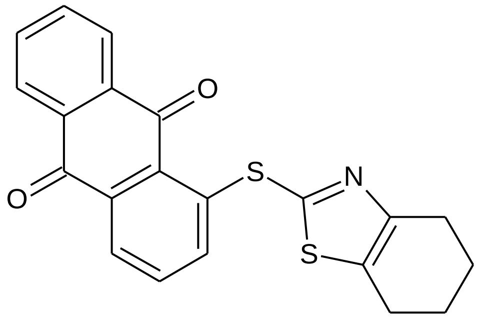

(a)

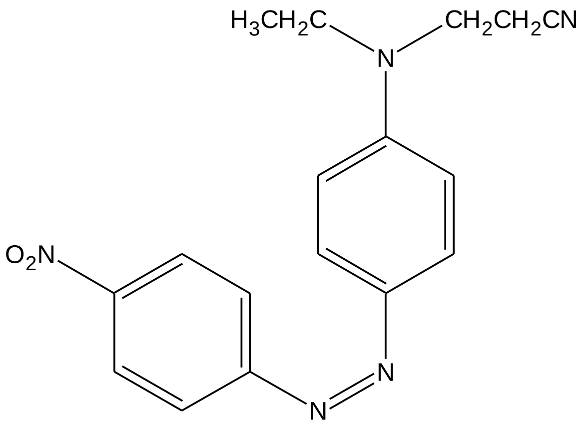

(b)

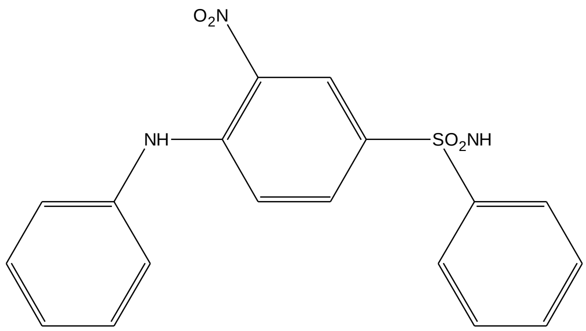

(c)

Figure 2.6 (a) CI Disperse Red 121, (b) CI Disperse Red 50 and (c) CI Disperse Yellow 42

2.3 STANDARDISED WASTEWATER TREATMENT METHODS

In surface water different compounds are present that must be removed if drinking water is to be produced. The compounds can be subdivided into:

- Suspended solids

- Colloidal solids

- dissolved solids.

Suspended solids have a diameter larger than 10 – 6 m, colloidal solids between 10 – 9 and 10 – 6 m and dissolved solids smaller than 10 – 9 m. Particles with a diameter larger than 10 – 5 m, and a specific density larger than 2,000 kg/m^3 will settle in water. Smaller particles will also settle, but more slowly. To be removed, particles that are smaller than 10 – 5 m must be made larger or heavier. The latter is impossible and, therefore, removal is only possible by increasing the particle size. During the coagulation and flocculation process, coagulants and flocculants are added to the water to aid in floc formation (Figure 2.7). These flocs are precipitates in water, wherein small particles are incorporated [7, 34].

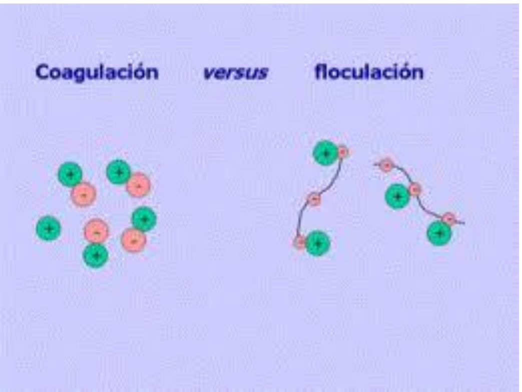

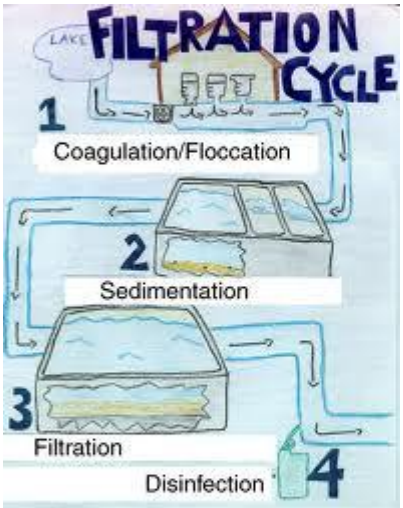

(a) (b)

Figure 2.7 coagulation vs. flocculation and (b) schematic of coagulation and flocculation process

To express the concentration of compounds in water, sum parameters are used. The most important sum parameters for surface water are “suspended solids” concentration (dry weight), “turbidity,” “natural organic matter” (expressed in TOC/DOC) and “colour.” “Suspended solids” concentration and turbidity are caused by colloidal particles (order of magnitude 0.1 - 10 μm). Colloidal particles are negatively charged and repulse each other.

Colour is caused by humic substances (order of magnitude 0.01 μm) mainly textile dyestuffs. The charge of humic substances (and thus the removal) is dependent upon the pH of the water.

2.3.1 Coagulation

To remove particles present in water, the particles must be incorporated into flocs. These flocs will be formed after dosing coagulant. In the Netherlands iron chloride ($FeCl_3$) is frequently used as the coagulant. Alternatively, aluminium sulphate can be applied. Iron chloride is easy to dissolve in water; the solubility product (Ksp) is 27.9 $mol^4 \cdot l^{-4}$,Consequently 162 mg $FeCl_3$ can be dissolved in one litre of water, resulting in 55.8 mg/l Fe^{3+} and 106.5 mg/l Cl.

The OH^- ions play an important role in coagulation. Fe^{3+} - and OH^- ions precipitate, because the solubility product of iron hydroxide is low and they precipitate into $Fe(OH)_3$ flocs. In electrostatic coagulation, positively charged ions approach the negatively charged colloids. In the diffusive layer around the colloid, the positively charged ions accumulate, destabilizing the colloid and can collide with other particles forming removable flocs [35].

2.3.4 Flocculation

The polymers can destabilize the colloidal particles through charge neutralization, electrostatic patch, bridging, or depletion flocculation. It has been accepted that the bridging mechanism is operating in the flocculation by non-ionic polymers [7, 35].

Flocculation is an important process in many industrial applications. Flocculation refers to a process where a solute comes out of solution in the form of floc. The term is also used to refer to the process by which fine particulates are caused to clump together into floc [7]. The floc may then float to the top of the liquid, settle to the bottom of the liquid. In geology, flocculation is a condition in which clays, polymer or other small charged particles become attached and form a flock.

2.4 TITANIUM OXIDE

2.4.1 History of TiO_2

Titania exists in a number of crystalline forms the most important of which are anatase and rutile. Pure titanium dioxide does not occur in nature but is derived from ilmenite or leuxocene ores. It is also readily mined in one of the purest forms, rutile beach sand. These ores are the principal raw materials used in the manufacture of titanium dioxide pigment [9, 10].

Titanium dioxide is one of the most important transition metal oxides on earth for its environmental applications. It has remarkable physical and chemical properties, biological inertness, nontoxicity, photostability and cost effectiveness, which makes it suitable for use for photocatalysis as well as gas sensors, photochromic devices and dye-sensitised TiO_2 solar cells, and also which can convert solar energy into chemical energy. The large specific area is responsible for high photocatalytic activity [11].

Titanium element was discovered in 1791 in England by William Gregor, who spent most of his time studying mineralogy. On his discovery he first called the mineral menachanite before discovering after four years that there was a new chemical element this mineral, which he then named Titanium after the Titans (humongous monsters which ruled in Greek mythology).

Since the development of carbon nanotubes, more focus has been on this unique low-dimensional nanostructured material because of its attractive various physical and chemical functions which arise from the synergy of low-dimensional nanostructure and anisotropy of carbon network, thus known as graphene structure. Various inorganic nanoturbular materials have been reported in non-oxide compounds (boron nitride and molybdenum disulphide), in oxides (titanium oxides) and natural minerals like imogolite [10].

2.4.2 Properties

Rutile, brookite and anatase are minerals composed of titanium dioxide. Three distinct titanium dioxidepolymorphs: rutile - a tetragonal mineral usually prismatic habit, often twinned; octahedrite or anatase - tetragonal mineral octahedral habit, and brookite - orthorhombic mineral (Figure 2.8). How octahedrite and brookite are relatively rare minerals. The size dependence of the stability of various TiO_2 phases has recently been reported. Rutile is the most stable phase for particles above 35 nm in size. Anatase is the most stable phase for nanoparticles below 11 nm. Brookite has been found to be the most stable for nanoparticles in the 11- 35 nm range. These have different activities for photocatalytic reactions, as summarized later, but the precise reasons for differing activities have not been elucidated in detail. Most practical work has been carried out with either rutile or anatase [18, 27].

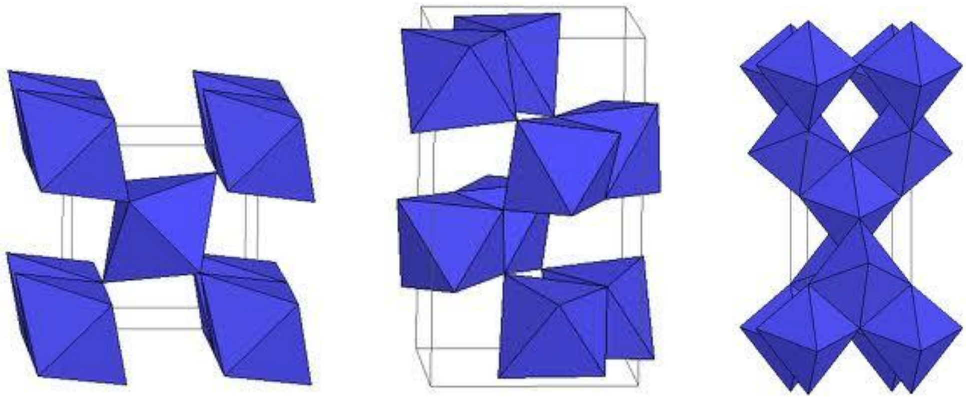

(a) **(b)** **(c)**

(a) **(b)** **(c)**

Figure 2.8 Crystal structures of (a) rutile, (b) brookite and (c) anatase

Rutile has the highest refractive index of any known mineral and also exhibits high dispersion. Table 2.2 and 2.3 show the chemical, physical and optical properties. Finely powdered rutile is a brilliant white pigment, and is used in paints, or plastics, papers, dishes and other applications that call for clear white. Titanium dioxide pigment is one of the largest worldwide use of titanium, while it is not currently economic benefit titanium metal from rutile. Nanoscale particles of rutile are transparent to optical light, but remain highly reflective to UV light and hence are used in sunscreens.

Table 2.2 The chemical and physical properties of TiO_2 at ambient temperature and atmospheric pressure.

Properties	
Molecular formula	TiO_2
Molar mass	79.87 g/mol
Appearance	White solid
Density	4.23 g/cm^3
Melting point	1870 °C (3398 °F)
Boiling point	2972 °C (5381.6 °F)
Solubility in other solvents	Insoluble

Table 2.3 Optical properties of anatase and rutile

Phase	Refractive Index	Density	Crystal structure
Anatase	2.49	3.84	Tetragonal
Rutile	2.903	4.26	Tetragonal

Rutile is the most stable form of titanium dioxide on a macroscopic scale and is produced at the highest temperatures, with brookite being formed at lower temperatures and octahedrite (anatase) being formed at even lower temperatures.

2.4.3 P25 Degussa

The TiO2 powder (Degussa, P-25), which is a standard material in the field of photocatalytic reactions, contains anatase and rutile phases in a ratio of about 3: 1.

The average sizes of the anatase and rutile elementary particles are 85 and 25 nm, respectively. P-25 (Degussa) has been a standard material, which has a relatively large surface area (49 m^2g^{-1}). Interestingly, the P-25 powder consists of anatase and rutile phases [12].

Because the P-25 powder shows high activity for many kinds of photocatalytic reactions, it has been used in many studies. In most studies, however, the effects of the mixed phases and the morphology have not been discussed in relation to the activity. TEM images of the P-25 powder clearly indicate that the anatase and rutile particles exist separately by forming their agglomerates, as shown in Figure 2.9.

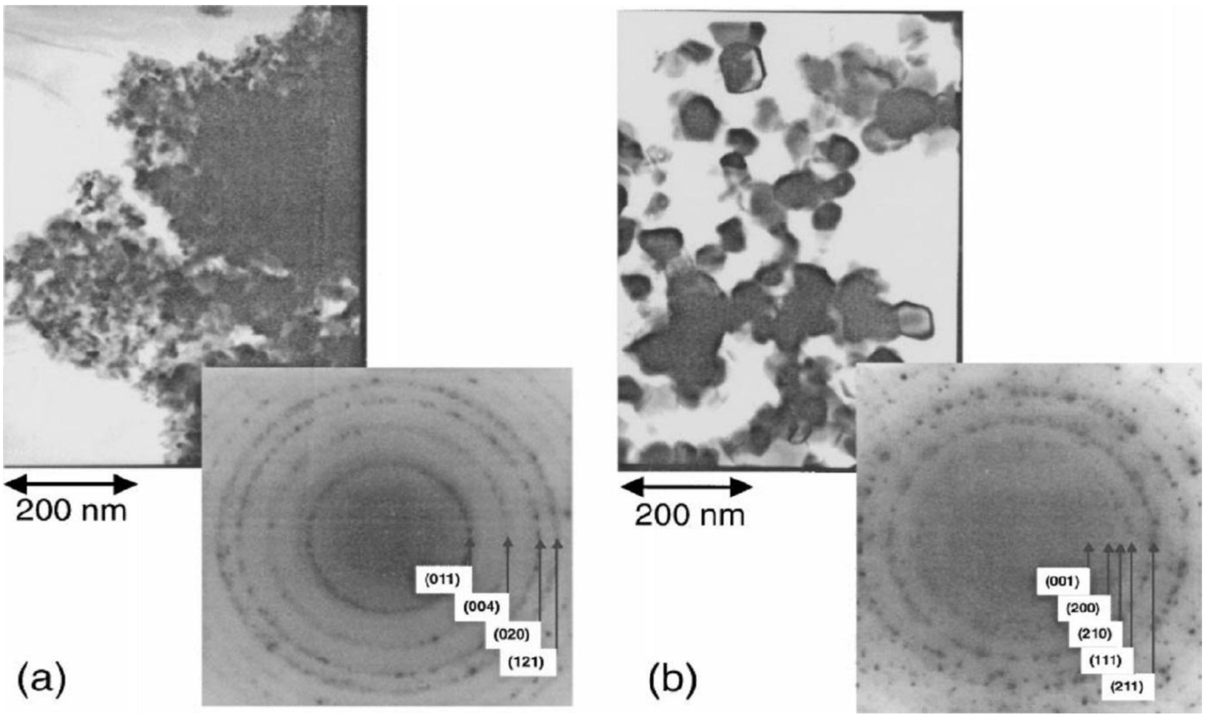

Figure 2.9 TEM photographs and electron diffraction patterns of the P-25 powder in the regions of (a) the anatase phase and (b) the rutile phase [12]

The crystal structures were assigned from the electron diffraction patterns. From these images, the average diameters of the anatase and rutile particles are estimated to be about 25 and 85 nm, respectively. By careful observation, we found amorphous particles in addition to the anatase and rutile particles, as shown in Fig.

2.9 P25 crystals are rounded, roughly spherical particles with an average diameter of 40 nm [15].

The P-25 powder is manufactured by the Aerosil process, by which titanium tetrachloride is subjected to hydrolysis in the vapour phase at an elevated temperature [13, 14]. Calibration curves for to determine the ratio of anatase, rutile and amorphous phase shown in Figure 2.10. During this process, the growth of particles is quenched when the particles (or the agglomerates) reach a certain size, since the grown particles (or the agglomerates) are removed from the reaction zone because of their increased weight [12].

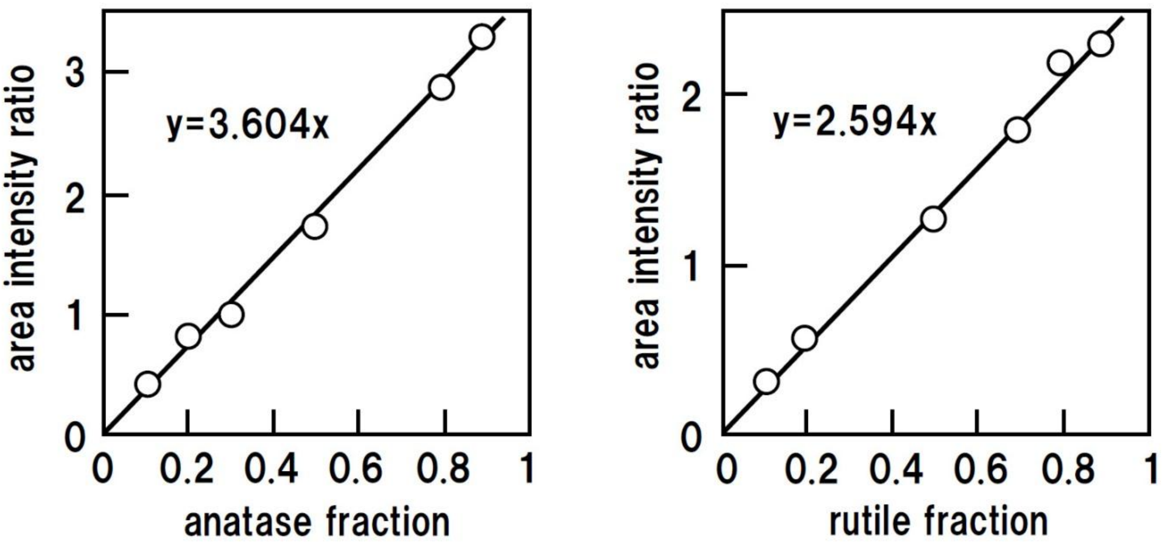

Figure 2.10 Calibration curves for the X-ray diffraction peaks were obtained to determine the ratio of anatase, rutile and amorphous phase [16].

2.5 PHOTOCATALYSIS

2.5.1 History of photocatalysis

Generally photo-catalysis is defined as "acceleration by the presence of as catalyst". A catalyst does not change in itself or being consumed in the chemical reaction. This definition includes photosensitization, a process by which a photochemical alteration occurs in one molecular entity as a result of initial absorption of radiation by another molecular entity called the photosensitized [26].

According to Akira Fujishma, 2005, Photocatalysis is generally thought of as the catalysis of a photochemical reaction at a solid surface, usually a semiconductor. This simple definition, while correct and useful, however, conceals the fact that there must be at least two reactions occurring simultaneously, the first involving oxidation, from photogenerated holes, and the second involving reduction, from photogenerated electrons. Both processes must be balanced precisely in order for the photocatalyst itself not to undergo change, which is, after all, one of the basic requirements for a catalyst [27].

The earliest work at the University of Lugano (Switzerland), reported in 1921 that titania is partially reduced during illumination with sunlight in the presence of an organic compound such as glycerol, the oxide turning from white to a dark colour, such as grey, blue or even black It has been recognized for quite a long time that titania-based exterior paints tend to undergo ``chalking'' in strong sunlight. This effect was recognized to result from the actual removal of part of the organic component of the paint, leaving the titania itself exposed. The photo-induced reduction was measured as a loss of reflectivity, due to the discoloration of the powder upon reduction, presumably to various oxygen-deficient forms, all the way to Ti_2O_3. The author proposed a cyclic redox process in which the titania was reduced while the organic paint components were oxidized, followed by re-oxidation of the titania by oxygen from the air. The changes experienced by the titania were recognized to be completely reversible, while those experienced by the organic paint were recognized to be irreversible, leading to the formation of water-soluble organic acids and CO_2.
In 1958, Kennedy et al., at the University of Edinburgh, studied the photo-adsorption of O_2 on TiO_2 in order to try to more fully understand the photocatalytic process [28]. They concluded that electrons were transferred to O_2 as a result of photoexcitation, and the resulting reduced form of O_2 adsorbed on the TiO_2 surface. They found also a correlation between the ability of the TiO_2 sample to photocatalytically decomposes chlorazol sky blue and the ability to photo-adsorb O_2 [27].

In further work at the University of Edinburgh, McLintock and Ritchie, using gas-phase adsorption measurements, studied the photocatalytic oxidation of ethylene and propylene at TiO2 [29]. This study is one of the first that we have found that shows that it is possible to oxidize organic compounds completely to CO_2 and H_2O:

$C_2H_4 + 3O_2 \rightarrow 2CO_2 + 2H_2O$: (1)

The mechanism was proposed to involve the production of superoxide from oxygen:

$O_2 + e^- \rightarrow O_2^{\bullet -}$ (2)

Frank and Bard were the first ones to propose that illuminated TiO_2 could be used for the purification of water via the photocatalytic decomposition of pollutants. They suggested that cyanide and sulphite could be photocatalytically oxidized to cyanate and sulphate, respectively [27]. The Bard group also proposed photocatalysis as a way to remove toxic metals from wastewater. For a period of several years, the photocatalysis area continued to expand as a technology for both the selective oxidation of organic compounds and the unselective oxidation of organic compounds for purposes of water purification and, to some extent, also air purification [30 – 33].

2.5.2 Mechanism of Photocatalysis

When photocatalyst titanium dioxide (TiO2) is irradiated by light energy greater than the band gap, separating the vacant conduction band (CB) and filled valence band (VB), the electron in VB is excited into CB and results in the formation of an excited electron (e^-) and a positive hole (h^+) pair (Figure 2.11). This stage is referred as the semiconductor's 'photo-excitation' state. Wavelength of the light necessary for photo-excitation is: 1240 / 3.2 eV = 388 nm [19, 21, 25, and 26].

1240 = (Planck's constant, h) and 3.2 eV = band gap energy

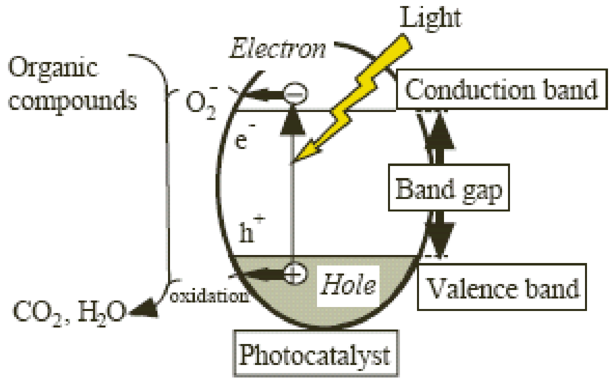

Figure 2.11 Mechanism of Photocatalysis

The positive-hole of titanium dioxide breaks apart the water molecule to form hydrogen gas and hydroxyl radical. The negative-electron reacts with oxygen molecule to form super oxide anion.

These e^- and h^+ reduce and oxidize respectively chemical species on the surface of photocatalyst, unless they recombine to give no net chemical reaction but heat. The chemical structure of the semi-conducting material remains unchanged if equal numbers of e^- and h^+ are consumed for chemical reaction. The apparent rate of the photocatalytic reaction depends on the photocatalyst, because efficiency of utilisation of incident or absorbed light energy is generally smaller than unity (the quantum efficiency can vary from unity to zero by changing the photocatalyst). In this sense one can define photocatalytic activity as the absolute or relative rate of photocatalytic reaction [19].

The photogenerated electrons could reduce the dye or react with electron acceptors such as O_2 adsorbed on the Ti(III)-surface or dissolved in water, reducing it to superoxide radical anion $O_2^{\bullet -}$. The photogenerated holes can oxidize the organic molecule R to form R^+, or react with OH^- or H_2O oxidizing them into $OH^\bullet$ radicals. Together with other highly oxidant species (peroxide radicals) they are reported to be responsible for the heterogeneous TiO_2 photodecomposition of organic substrates such as dyes. According to this, the relevant reactions at the semiconductor surface causing the degradation of dyes can be expressed as follows:

$TiO_2 + hv\ (UV) \rightarrow TiO_2\ (e_{CB}^- + h_{VB}^+)$ (3)

$TiO_2 (h_{VB}^+) + H_2O \rightarrow TiO_2 + H^+ + OH^\bullet$ (4)

$TiO_2 (h_{VB}^+) + OH^- \rightarrow TiO_2 + OH^\bullet$ (5)

$TiO_2 (e_{CB}^-) + O_2 \rightarrow TiO_2 + O_2^{\bullet -}$ (6)

$O_2^{\bullet -} + H^+ \rightarrow HO_2^\bullet$ (7)

Dye + $OH^\bullet \rightarrow$ degradation products (8)

Dye + $h_{VB}^+ \rightarrow$ oxidation products (9)

Dye + $e_{CB}^- \rightarrow$ reduction products (10)

The resulting $^\bullet OH$ radical, being a very strong oxidizing agent (standard redox potential +2.8 V) can oxidize most of azo dyes to the mineral end-products. Substrates not reactive toward hydroxyl radicals are degraded employing TiO_2 photocatalysis with rates of decay highly influenced by the semiconductor valence band edge position. The role of reductive pathways [Eq. (10)] in heterogeneous photocatalysis has been envisaged also in the degradation of several dyes but in a minor extent than oxidation [17].

Most experimental results indicated that the destruction rates of photocatalytic oxidation of various dyes over illuminated TiO_2 fitted the Langmuir–Hinshelwood (L–H) kinetics model [20]:

$$r = \frac{dC}{dt} = \frac{kKC}{1 + kC}$$

Where *r* is the oxidation rate of the reactant (mg/l min), *C* the concentration of the reactant (mg/l), *t* the illumination time, *k* the reaction rate constant (mg/l min), and *K* is the adsorption coefficient of the reactant (l/mg). When the chemical concentration *C*o is a millimolar solution (*C*o small) the equation can be simplified to an apparent first-order equation:

$$\mathrm{Ln}\left(\frac{Co}{C}\right) = kKt = kapp.t \text{ or } Ct = Coe^{-k}app.t$$

A plot of ln *C*o/*C* versus time represents a straight line, the slope of which upon linear regression equals the apparent first-order rate constant *k*app. The L–H model was established to describe the dependence of the observed reaction rate on the initial solute concentrations.

It has been agreed, with minor doubts that the expression for the rate of photomineralization of organic substrates such dyes with irradiated TiO2 follows the Langmuir–Hinshelwood (L–H) law for the four possible situations:

(a) The reaction takes place between two adsorbed substances,
(b) The reaction occurs between a radical in solution and an adsorbed substrate molecule,
(c) The reaction takes place between a radical linked to the surface and a substrate molecule in solution, and
(d) The reaction occurs with the both of species being in solution.

In all cases, the expression for the rate equation is similar to that derived from the L–H model, which has been useful in modelling the process, although it is not possible to find out whether the process takes place on the surface in the solution or at the interface [20].

Kaneko, Okura (2002); however suggested that it is wrong to base the linear relation between the rate of photocatalytic reaction and the amount of surface adsorbed on the surface to L-H mechanism, because this mechanism involves the surface reaction of two kinds of adsorbed species, of which is not realized in photocatalytic reaction system. In photocatalytic reaction systems, only a small amount of the photocatalyst particles or an outer part of bulk of the entire material can absorb incident photons, and the rest does not take part in the reaction. However the total number of absorbed photons should be constant if the sufficient amount of photocatalyst absorbs all the incident photons and thus the total number of e^- and h^+ pairs is expected to be independent on specific surface area [19].

3. EXPERIMENTS

3.1 METHODS AND MATERIALS

The main objective of the experimental part of this thesis work is to remove colour on textile wastewater containing different classes of dyes by UV/TiO_2 photo-catalysis and compare this method to other standardized methods (coagulation and flocculation). The dyes treated are the azo-dyes (Disperse Red 50,Direct Yellow 44, Reactive Blue 19, Reactive Blue 4, 1:1 metal complex Acid Blue 158, 1:2 metal complex Acid Red 213 and Acid Yellow 11), anthraquinone dyes (Disperse Red 121), oxazine dyes (Direct Blue 106) and nitro dyes (Disperse Yellow 42).

3.1.1 Classical Way (coagulation)

- 50 g/l solutions of $FeSO_4$, $Ca(OH)_2$ and Na_2CO_3 prepared
- 5 ml of ferrous sulphate ($FeSO_4$) and calcium hydroxide [$Ca(OH)_2$] added in 30 ml dye solution of 0.1 g/l concentration
- Alkali pH = 8.5 controlled by the addition of sodium carbonate (Na_2CO_3)
- The flock settling volume recorded in 5 minute time intervals for one hour.

3.1.2 Flocculation

- 100 g/l solution of flocculating agent Texaflok 32 (for medium concentrated dye solutions – supplied by Inotex Czech Republic) was prepared
- 4 different dyestuffs selected, each with 0,1 g/l concentration – Disperse Red 121, Reactive Blue 4, Acid Yellow 11 and Acid Blue 158 (1:1 metal complex dye)
- Then from each dyestuff 3 x 30 ml solution separated into three graduated cylinders (Figure 3.1) for the application of different amounts of Texaflok 32 (0.1, 0.2 and 0.3 ml)
- Na_2CO_3 added to control pH to 8.5
- The flock settling volume recorded in 5 minute time intervals for one hour.

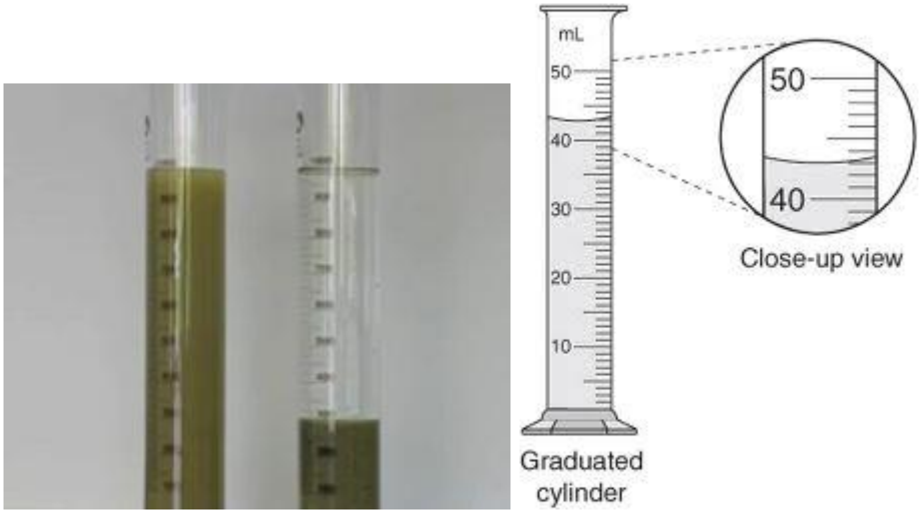

Figure 3.1 Apparatus used in flocculation and coagulation – a 50 ml graduateed cylinder, with a height of 20 mm and diameter of 26 mm.

3.1.3 Classical Way on simulated dye-baths

- Simulated dye-baths were prepared by addition of chemicals suitable for these dyes.
- For direct and reactive dyes NaCl and Na_2CO_3 to control the pH to 8.5,
- for acid and metal complex dyes HCOOH was added to get to pH 4.5
- followed by the addition of 5 ml of ferrous sulphate and calcium hydroxide
- The flock settling volume recorded in 5 minute time intervals for one hour.

3.1.4 Photo-catalysis

The primary step in photo degradation is the formation of an excited electron (e^-)-positive hole (h^+) pair. This stage is referred as the semiconductor's 'photo-excitation' state. Wavelength of the light necessary for photo-excitation is: 1240 / 3.2 eV = 388 nm.

METHOD

HOMOGENISATION

Dyestuff solutions (100 ml) of 0.1 g/l concentration and 0.1 g TiO2 (P25 Degussa) were prepared. The homogenisation of dye solution and TiO2 powder effected by the use of Ultrasonic Supersonic supplied by Bandelin (Figure 3.2). This helps in the reduction of soft and hard particles and/or agglomerates. The process was carried for 60 seconds at ultrasonic capacity of 50 KHz.

The homogenization is based on cavitation. When liquids are exposed to intense ultrasonication sound waves propagate through the liquid causing alternating high-pressure and low-pressure cycles (approx. 20000 cycles/sec.). During the low-pressure cycle, high-intensity small vacuum bubbles are created in the liquid, as the liquid vapour pressure is attained. When the bubbles reach a certain size, they collapse violently during a high-pressure cycle. During this implosion very high pressures and high speed liquid jets are generated locally. The resulting currents and turbulences disrupt particle agglomerates and lead to violent collisions between individual particles.

Figure 3.2 Ultrasonic Supersonic supplied by Bandelin

UV IRRADIATION

Homogenised solutions (30 ml from each sample) irradiated with ultraviolet light (UV) at ambient temperature. The process carried out using TL' 6W /05 Philips fluorescent lamps with UV irradiant intensity of 3120 μW/cm^2 at a distance of 5 cm from the treated sample for 60 minutes (Figure 3.3). A magnetic stirrer (400 rpm) used during UV irradiation of the 30 ml homogenised solution in a petri dish of 70 mm diameter and 15mm for 60 minutes for each solution.

Figure 3.3 TL’ 6W /05 Philips fluorescent lamps with UV irradiant intensity of 3120 μW/cm^2

IMAGES

Images for analysis with Image J software were taken by Cannon camera (in five minutes intervals for 60 minutes) at a distance of 19.5 cm from the sample, using a focal distance of 35 mm. Some specifications of the camera are:

- Electro Optical System (EOS) – 400D + (Electro focus 18 – 55 mm)
- Zoom Lens – 1:3.5 – F5.6
- Filter – B + W 58 KR – 1.5 skylight 1.1 x MRC
- Exposure Time – 1/160

Image J software is based on RGB system starting with black and as colours are added, the amount of emitted light is increase (additive colours = Red, Blue and Green); with pixel values for every pixel in each channel (digital cameras, computer display, etc.).

EVALUATION

Three standards used for the valuation of results: 0% - 100ml ionised water + 0.1g TiO_2 P25, 50 % - 50ml H_2O + 50ml dye solution (0.1g/l) + 0.1g TiO_2 P25 and 100% - 100 dye solution (0.1g/l) + 0.1g/l TiO_2 P25.All colours are displayed by varying pixel values. For a 24 bit colour image: White – R = 255, G = 255 and B =255; Black – R = 0, G = 0 and B =0; Pure Red – R = 255, G = 0 and B =0; Green – R = 0, G = 255 and B =0 and for Blue – R = 0, G = 0 and B =255.

3.2 RESULTS AND DISCUSSION

3.2.1 Classical Way (Coagulation)

Particles finer than 0.1 µm (10^{-7}m) in water remain continuously in motion due to electrostatic charge (often negative) which causes them to repel each other. Once their electrostatic charge is neutralized by the use of coagulant chemical, the finer particles start to collide and agglomerate (combine together) under the influence of Van der Waals's forces. These larger and heavier particles are called flocs.

Table 3.1 shows the flock settling volume for different dyestuffs at pH 8.5 as a result of 5 ml $FeSO_4$ and $Ca(OH)_2$ (both 50 g/l concentration) added on 30 ml dyestuff solution. The azo dyes, Acid Yellow 11, Disperse Red 50, Direct Yellow 44 and Acid Red 213 showed 57 %, 57 %, 55 % and 54 % aggregate settling after one hour.

Table 3.1 Coagulation - flock settling volume for different dyestuffs

Time (min)	**SETTLING VOLUME (ml)**									
	Disp Yel 42	Disp Red 121	Disp Red 50	Reactive Blue 19	Reactive Blue 4	Acid Red 213	Acid Yel 11	Acid Blue 158	Direct Yel 44	Direct Blue 106
0	40	40	40	40	40	40	40	40	40	40
5	37.5	38	38	38	38	38	38	38	37.5	38
10	35.5	37	34.5	36.5	36.5	36.5	33.5	36.5	35.5	35
15	33.5	36	29	35	34.5	34	28	35	33.5	34.5
20	32	35	25	33.5	32.5	30	25.5	33.5	31	32.5
25	30	33.5	23	31.5	31	28	23.5	31.5	28	30.5
30	28	32	21.5	30	29	25.5	21.5	30	25.5	28.5
35	26.5	31	20.2	28	27	24	20.5	28	24	26.5
40	24	30	19.5	26.5	25.5	22.5	19.5	27	22.5	25
45	23	28.5	19	25	24	21.5	19	25.5	21	23.5
50	21.5	27	18	23	23.5	20	18	23.5	19.5	21.5
55	20	26	17.5	22.5	21.5	19	17.5	22.5	19	20.5
60	19	25	17	21.5	20	18.5	17	21.5	18	19.5

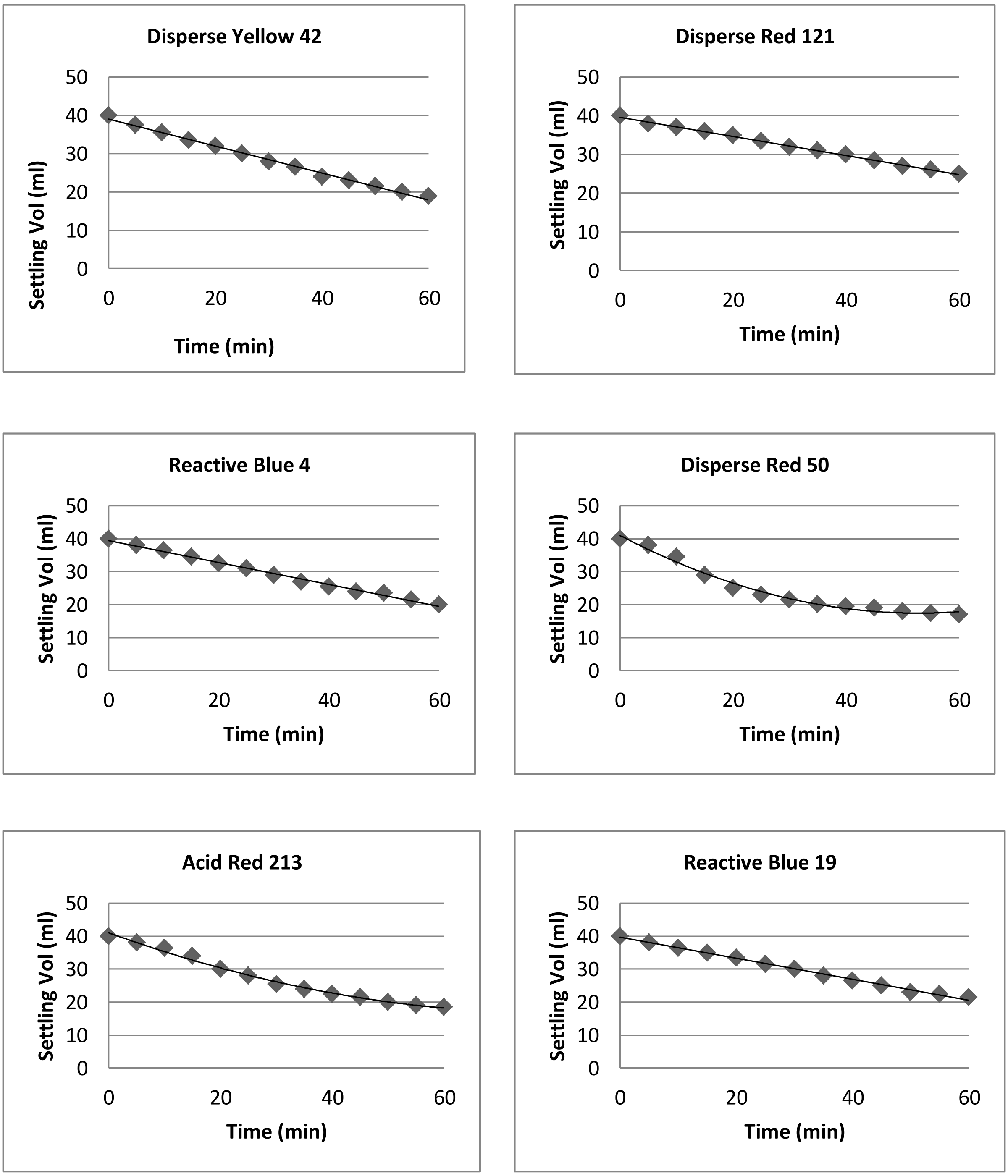

Figure 3.4 Effect of coagulation on different dyes (0.1 g/l) after 60 seconds

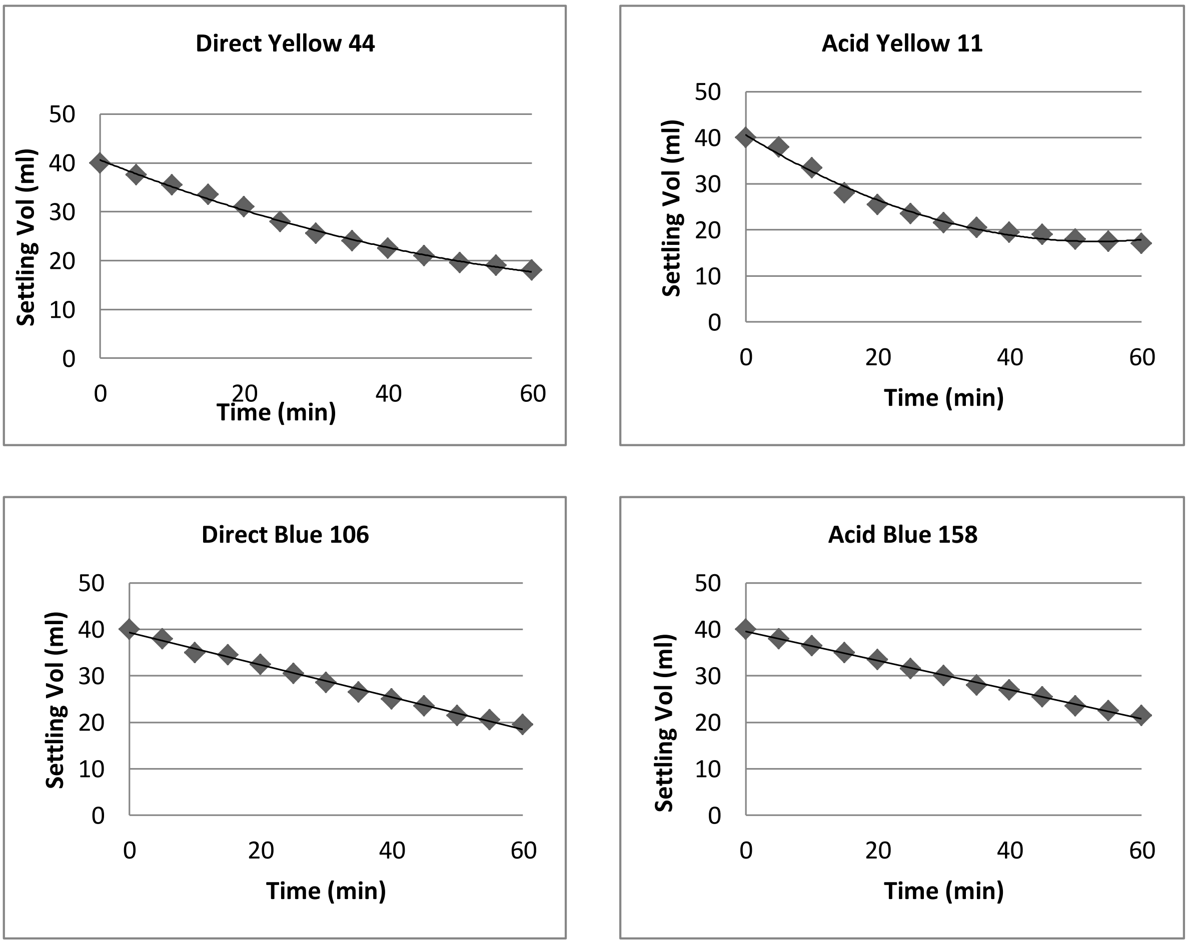

Figure 3.5 Effect of coagulation on different dyes (0.1 g/l) after 60 seconds

Table 3.2 VIS absorbency of coagulation treated dye solutions

Spectrophotometric Results			
	Wavelength (nm)	Absorbency	
Dyestuff		Before	After
Disperse Yellow 42	430	1.0672	0.03409
Disperse Red 121	584	0.99226	0.01509
Disperse Red 50	478	1.5759	0.037
Reactive Blue 19	592	0.97287	0.01039
Reactive Blue 4	598	0.77087	0.0157
Acid Red 213	544	0.77888	0.03119
Acid Yellow 11	392	1.9907	0.05579
Acid Blue 158	630	2.4596	0.01385
Direct Yellow 44	394	2.4983	0.34779
Direct Blue 106	592	1.2442	0.00555

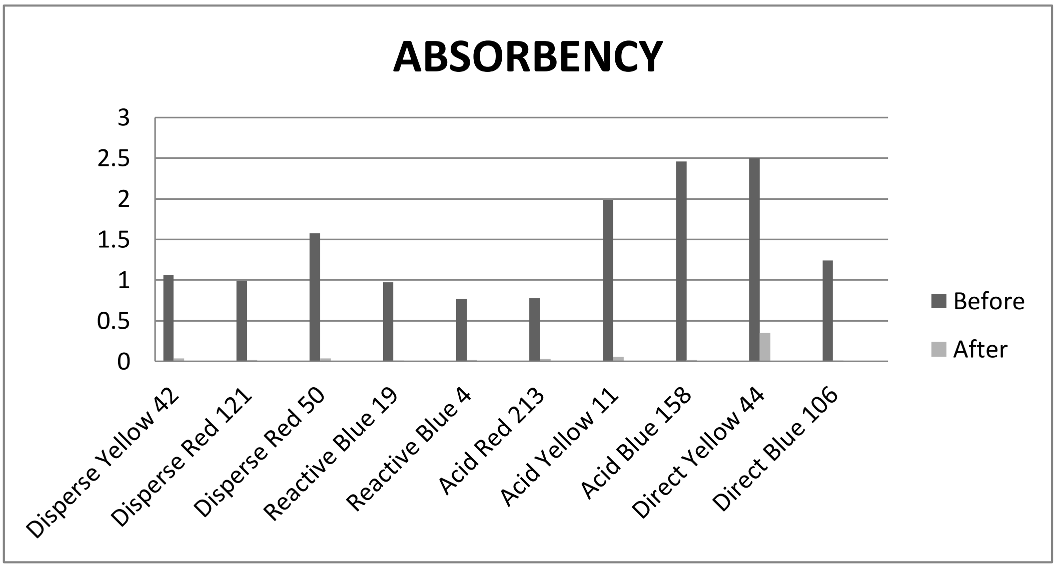

Figure 3.6 VIS absorbency of coagulation treated dye solutions

3.2.2 Flocculation

It has been indicated that polymers can destabilise the colloidal particles through charge neutralisation, electrostatic patch, and bridging or depletion flocculation. The bridging mechanism is operating in the flocculation by non – ionic polymers [9].

Table 3.3 Flocculation – flock settling volume for different dyestuffs

Flocculation Way														
Dyestuff	**Time (min)**	0	5	10	15	20	25	30	35	40	45	50	55	60
	Agent (ml)	**Settling Volume (ml)**												
Disperse Red 121	0.1	30.5	30.5	30	28	27	20	18	12	5	5	5	5	5
	0.2	30.5	30.5	30	28	26	20	17	12	5	5	5	5	5
	0.3	30.5	30.5	30.5	30	30	26	15	15	5	5	5	5	5
Reactive Blue 4	0.1	30.5	30.5	30.5	30	30	30	30	30	30	29	29	29	29
	0.2	30.5	30.5	30.5	30	30	30	30	30	30	30	30	30	30
	0.3	30.5	30.5	30.5	30	30	30	30	30	30	30	30	30	30
Acid Yellow 11	0.1	30.5	30.5	30.5	30.5	30.5	31	31	31	31	30.5	31	31	31
	0.2	30.5	30.5	30.5	30.5	30.5	31	31	31	31	30.5	31	31	31
	0.3	30.5	30.5	30.5	30.5	30.5	31	31	31	31	30.5	31	31	31
Acid Blue 158	0.1	30.5	30.5	30.5	30.5	30.5	31	31	31	31	30.5	31	31	31
	0.2	30.5	30.5	30.5	30.5	30.5	31	31	31	31	30.5	31	31	31
	0.3	30.5	30.5	30.5	30	30	30	30	30	30	30	30	30	30

Table 2.1 show the settling volume of different dyestuffs after 60 min of the flocculation process. The process showed to be more effective on the three types of disperse dyes: 1) Disperse Yellow 42 (nitro dye), 2) Disperse Red 121 (anthraquinone dye) and 3) Disperse Red 50; and achieving 84 % settling volume after 35 minutes while the settling volume of the other dyes range at 5% after 60 minutes.

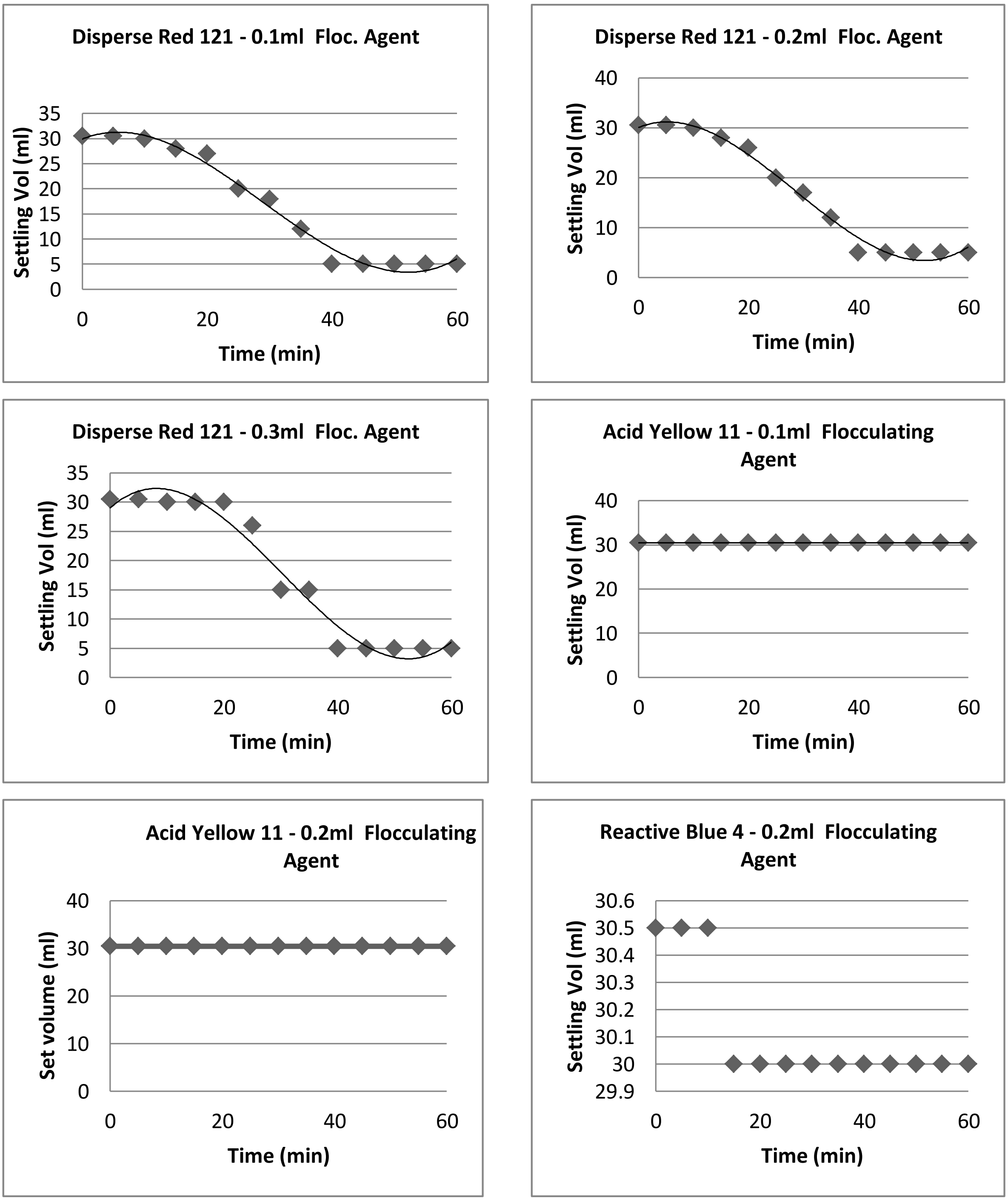

Figure 3.7 Effect of flocculation on different dyes (0.1 g/l) after 60 seconds

Table 3.4 VIS absorbency of flocculation treated dye solutions

SPECROPHOTOMETRIC RESULTS					
DYESTUFF	WAVELENGHT (nm)	ABSORBENCY			
		BEFORE	AFTER		
			Flocculating Agent (ml)		
			0.1	0.2	0.3
Disperse Red 121	584	0.99226	0.051	0.037	0.0605
Reactive Blue 4	598	0.77087	0.05	0.0715	0.0631
Acid Yellow 11	392	1.9907	2.348	1.8425	1.7088
Acid Blue 158	630	2.4596	0.42	0.1526	0.3994

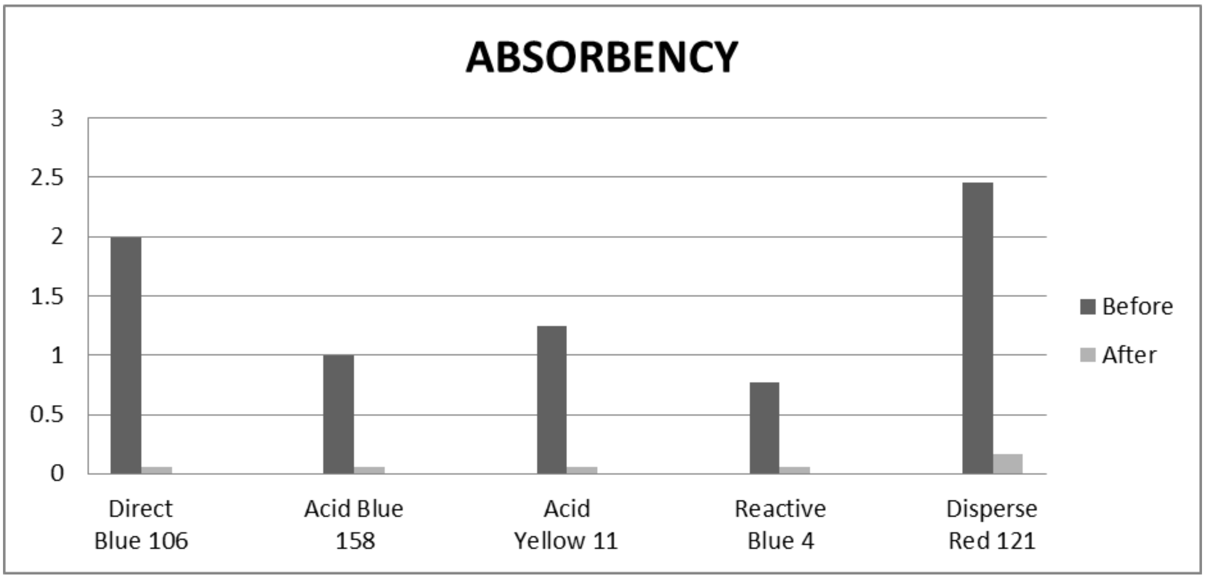

Figure 3.8 VIS absorbency of flocculation treated dye solutions

Filtration process done to in order perform the spectrophotometric absorbency test for the flocculation treated samples due to low settling rate of flocs.

3.2.3 Classical Way on Simulated Dye baths

Table 3.5 Flock settling volume during flocculation of simulated dye-bath samples

Time (min)	Settling Volume (ml)				
	Direct Blue 106	Acid Blue 158	Acid Yellow 11	Reactive Blue 4	Disperse Red 121
0	40.5	40.5	40.5	40.5	40.5
5	39	38	38.5	39	39
10	37.5	35	36	37.5	37.5
15	36.5	33	34.5	36.5	36
20	35.5	31.5	33	35.5	35.5
25	34	29.5	31	34	34.5
30	33	28	29.5	33	33.5
35	32	26.5	28	32	32.5
40	31	25	27	31	32
45	30	24	25.5	30	31
50	29	22.5	23	29	29.5
55	28	21	22	28	28.5
60	27	20	21	26.5	27.5

Settling of flocs after 60 min on coagulation process with simulated dye baths took longer as compared to standard dye solution (results on Figure 3.5, 3.6 and 3.9). For the simulated process: CI Acid Yellow 11 – 49 %, CI Acid Blue 158 – 53 %, CI Reactive Blue 4 – 35 %, CI Direct Blue 106 – 33 % and CI Disperse Red 121 – 32 %.

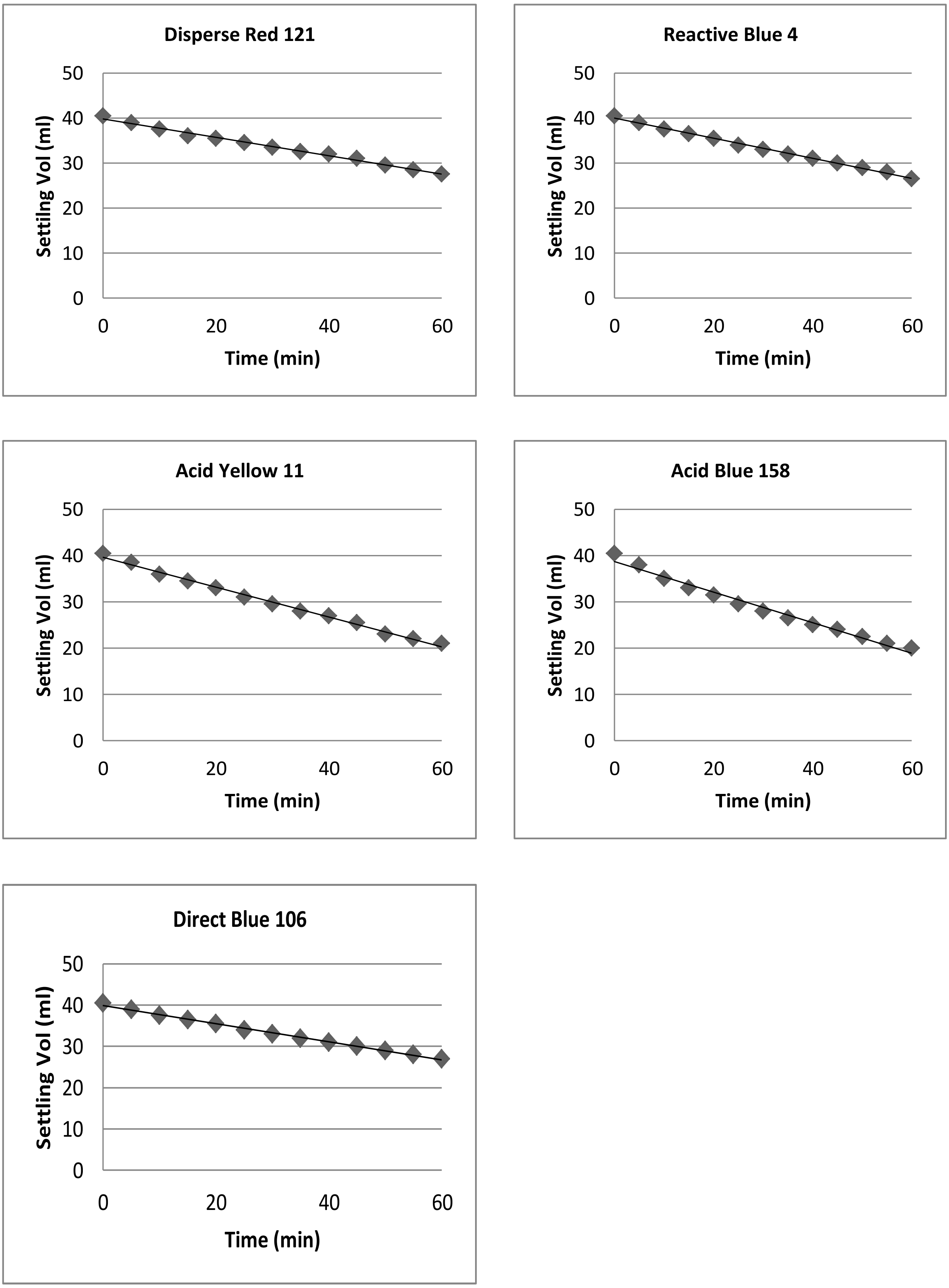

Figure 3.9 Effect of coagulation on simulated dyebaths (0.1 g/l) after 60 seconds

Table 3.6 VIS absorbency of treated dye solutions from simulated dye-baths

Spectrophotometric Results			
		Absorbency	
Dyestuff	Wavelength (nm)	Before	After
Direct Blue 106	592	1.0672	0.05922
Acid Blue 158	630	0.99226	0.161
Acid Yellow 11	392	1.5759	0.053
Reactive Blue 4	598	0.97287	0.053
Disperse Red 121	584	0.77087	0.058

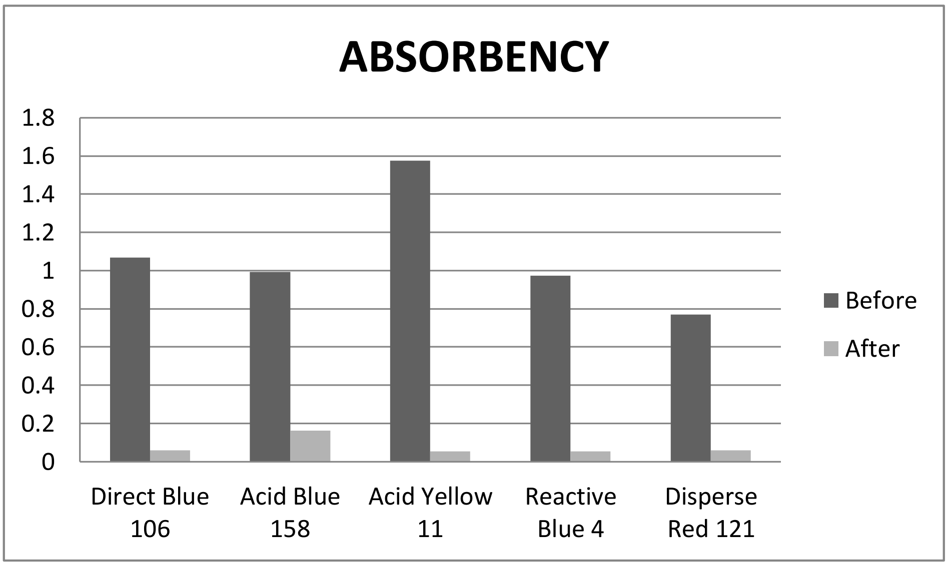

Figure 3.10 VIS absorbency of treated dye solutions from simulated dye-baths

Flocculation process at different concentrations of flocculating agent (Texaflok 32 – for medium concentrated dye solutions) was only effective on disperse dyes, achieving a settling volume of 95 – 98 % after 40 minutes (Figure 3.7).

3.2.4 Photo-catalysis

Table 3.7 Intensity data from Image J analysis, (a) CI Direct Blue 106 and (b) CI Acid Red 213

Time	Intensity		
	Red	**Green**	**Blue**
2	76.59	91.2	128.41
5	80.8	91.29	120.66
10	98.14	105.56	131.12
15	97.55	103.67	123.76
20	93.89	97.99	110.74
25	100.26	102.58	114.86
30	107.42	107.68	117.25
35	118.27	117.03	123.36
40	119.93	117.02	120.33
45	127.42	121.08	119.71
50	151.75	142.59	137.23
55	166.22	153.57	143.24
60	178.23	162.12	146.48

Time	Intensity		
	Red	**Green**	**Blue**
2	168.36	61.06	57.77
5	169.37	66.49	60.74
10	168.24	72.75	64.12
15	176.48	89.1	75.76
20	179.55	112.73	85.71
25	181.87	124.81	97.77
30	191.78	137.83	107.64
35	188.45	143.44	116.28
40	189.14	143.6	114.49
45	190.88	147.13	118.85
50	193.42	150.58	124.54
55	195.17	157.43	131.01
60	196.04	161.34	135.34

Standard	0%	50%	100%
Red	**211.41**	**114.06**	**74.96**
Green	192.88	121.49	88.09
Blue	167.7	152.66	130.33

(a)

Standard	0%	50%	100%
Red	211.41	196.39	167.72
Green	**192.88**	**88.08**	**60.75**
Blue	167.7	77.54	57.53

(b)

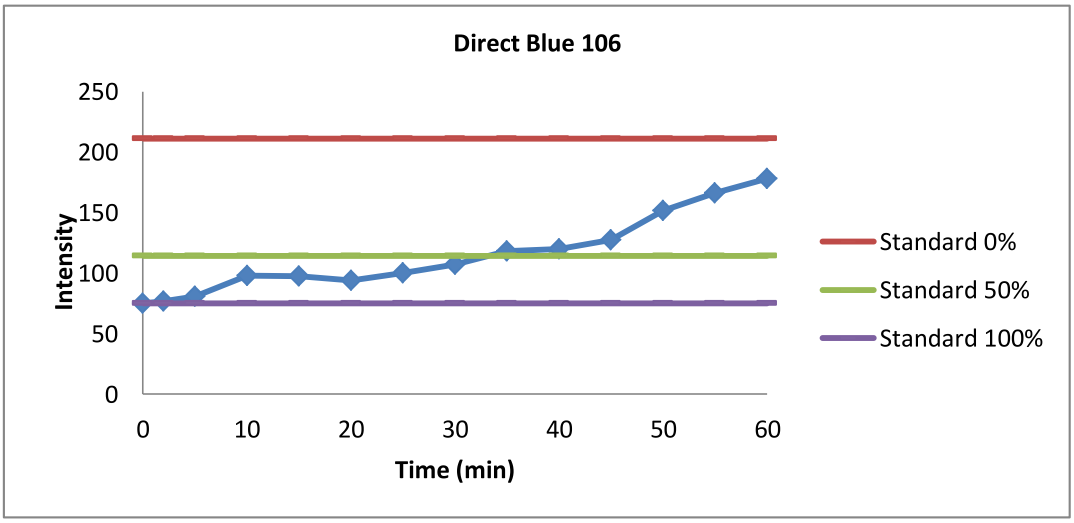

(a) (b)

Figure 3.11 Effect TiO_2 photocatalysis on CI Direct Blue 106, (a) dyestuff and TiO_2 solution before UV irradiation (standard 100%) and (b) UV irradiated sample after 60 minutes.

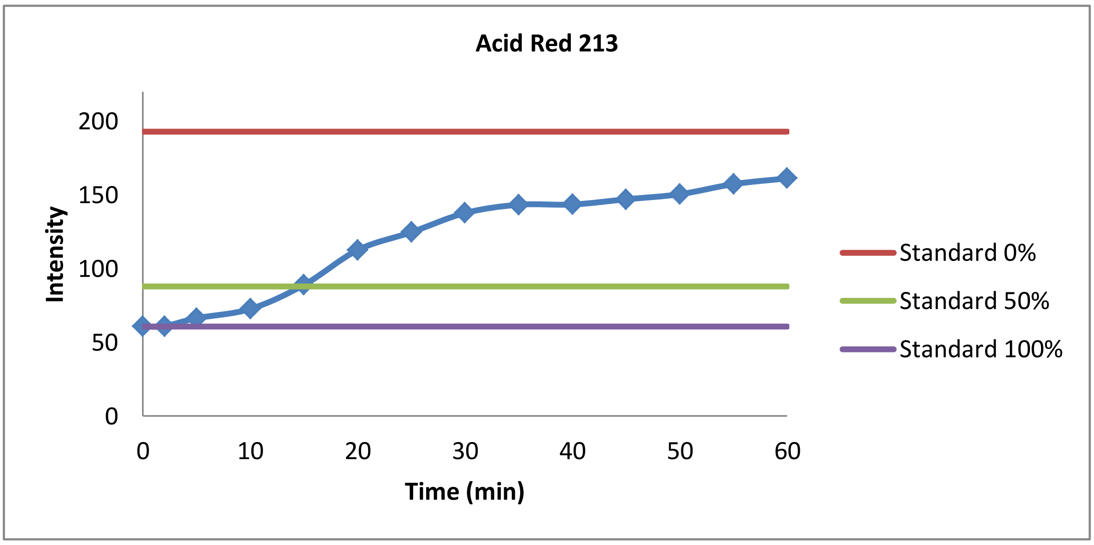

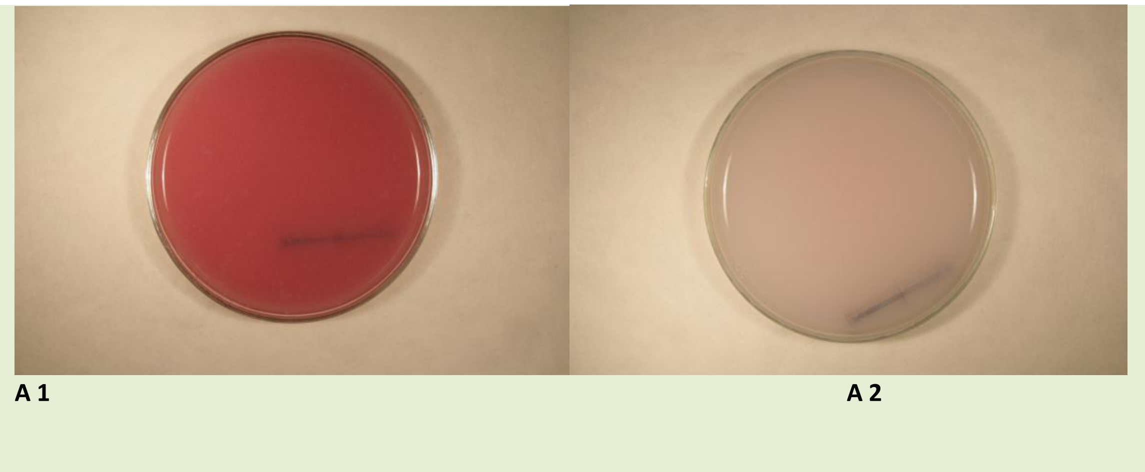

Figure 3.12 Effect TiO_2 photocatalysis on CI Acid Red 213, A1) dyestuff and TiO_2 solution before UV irradiation (standard 100%) and A2) UV irradiated sample after 60 min

Table 3.8 Intensity data from Image J analysis, (a) CI Acid Yellow 11 and (b) CI Disperse Yellow 42

Time	Intensity		
	Red	**Green**	**Blue**
2	210.04	186.28	52.8
5	204.45	172.45	48.17
10	206.8	169.34	45.91
15	205.9	167.67	44.43
20	208.73	169.85	48.6
25	207.63	169.17	48.58
30	205.63	165.63	47.99
35	212.68	175.84	63.41
40	210.9	172.91	63.39
45	204.61	164.7	62.86
50	204.6	165.79	63.67
55	206.5	169.94	64.55
60	207.18	170.91	66.09

Standard	**0%**	**50%**	**100%**
Red	211.41	210.47	214.1
Green	192.88	191.56	195.19
Blue	**167.7**	**88.31**	**68.19**

(a)

Time	Intensity		
	Red	**Green**	**Blue**
2	204.62	172.85	90.48
5	206.39	174.37	90.65
10	202.32	170.22	86.65
15	205.17	172.88	87.56
20	197.5	166.66	84.37
25	204.25	172.82	86.16
30	207.33	177.27	86.39
35	200.13	167.96	67.15
40	207.18	176.03	73.98
45	208.69	179.75	77.41
50	208.34	179.38	77.82
55	204.21	176.57	78.12
60	205.12	175.65	78.65

Standard	**0%**	**50%**	**100%**
Red	211.41	203.81	208.07
Green	192.88	178.99	177.57
Blue	**167.7**	**112.33**	**94.03**

(b)

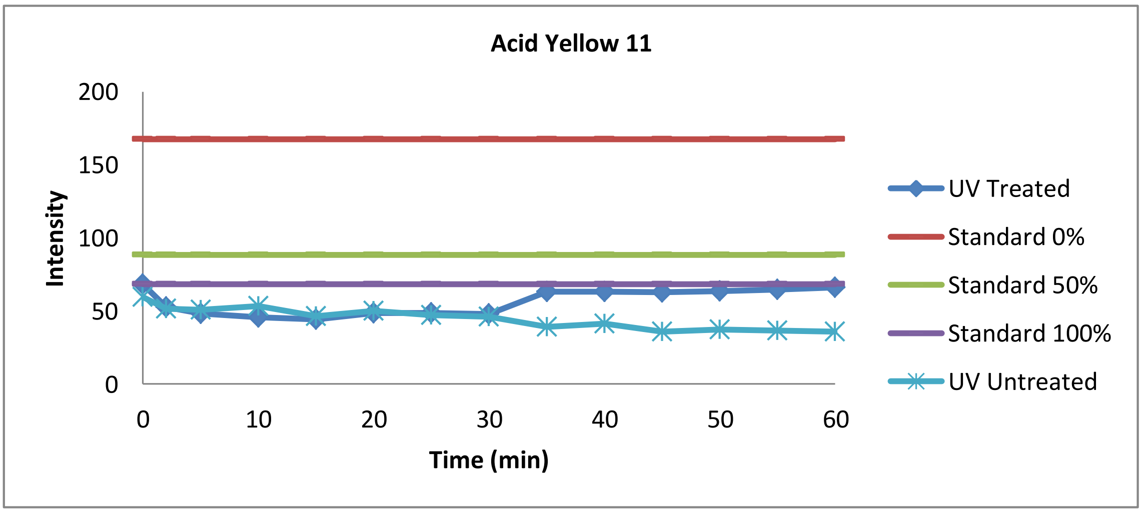

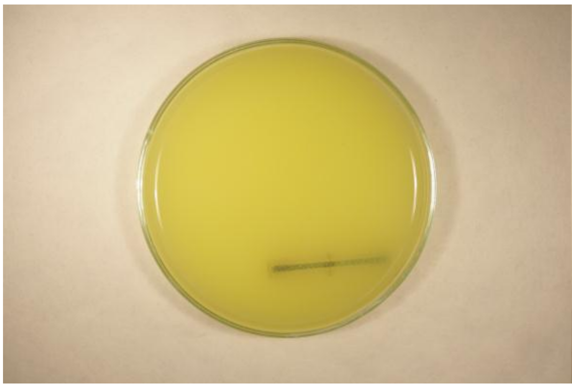

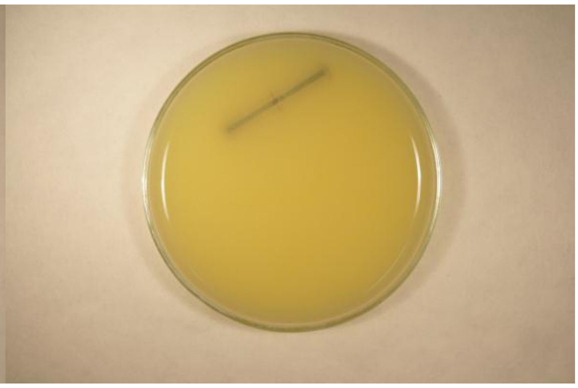

A 2 A 2

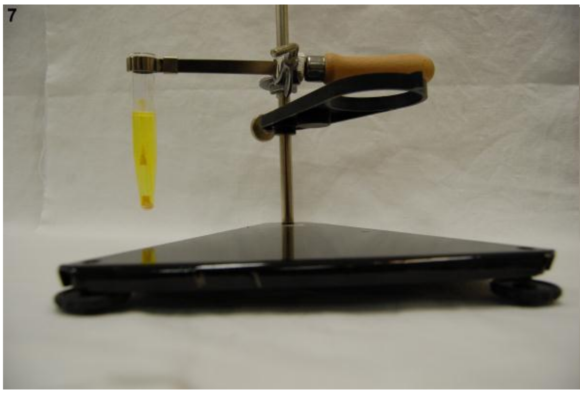

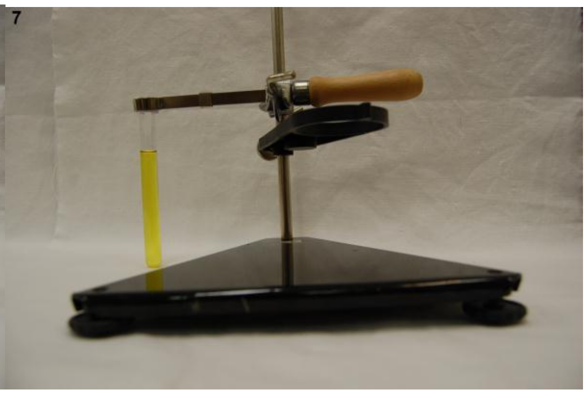

A 3 A 4

Figure 3.13 Effect TiO_2 photocatalysis on CI Acid Yellow 11, A1) dyestuff and TiO_2 solution before UV irradiation (standard 100%), A2) UV irradiated sample after 60 min, A3) UV treated sample after membrane filtration and A4) after centrifuge

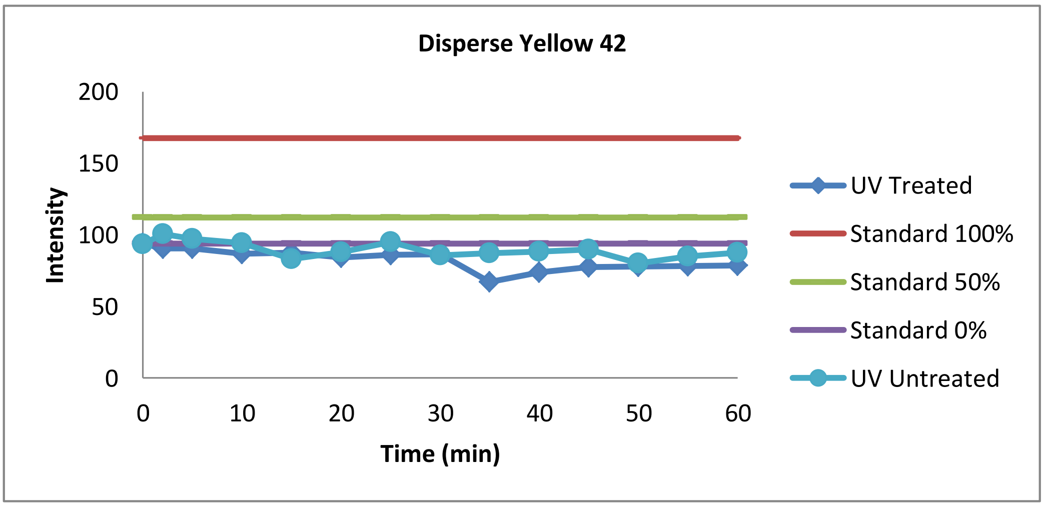

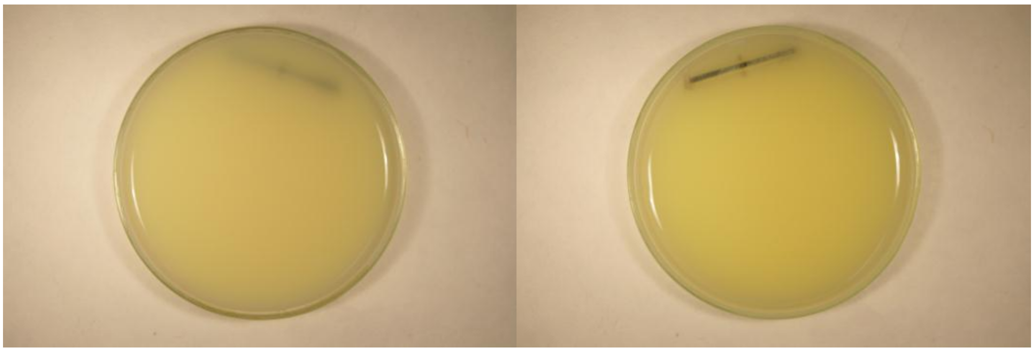

A 1 A 2

Figure 3.14 Effect TiO_2 photocatalysis on CI Disperse Yellow 42 (UV treated and untreated), A1) dyestuff and TiO_2 solution before UV irradiation (standard 100%) and A2) UV irradiated sample after 60 min

The treated and untreated CI Disperse Yellow 42 samples indicate similar trends, both being about 50 % darker than the 100% standard (Figure 3.14 and 3.15). The effect was common with all UV/TiO_2 and TiO_2 /VIS treated samples disperse dyes.

Table 3.9 Intensity data from Image J analysis, (a) CI Disperse Red 121 and (b) CI Disperse Red 50

Time	Intensity		
	Red	**Green**	**Blue**
2	172.95	87.62	96.21
5	174.11	88.15	96.46
10	173.05	87.68	96.29
15	173.39	87.82	96.5
20	175.77	89.1	97.74
25	175.36	88.82	97.74
30	178.5	88.5	97.71
35	172.6	75.42	84.52
40	171.66	72.47	81.5
45	162.91	67.93	75.89
50	178.13	78.22	87.31
55	167.33	69.71	77.12
60	164.39	68.03	75.82

Time	Intensity		
	Red	**Green**	**Blue**
2	153.9	75.69	59.61
5	154.98	75.98	59.37
10	153.5	75.09	58.69
15	150.81	72.83	56.8
20	151.59	73.31	56.81
25	149.35	72.04	56.86
30	146.91	69.43	52.99
35	149.54	71.85	56.83
40	147.21	62.74	45.83
45	139.03	53.65	35.44
50	139.16	54.52	34.91
55	134.42	51.78	34.23
60	136.91	52.71	35.06

Standard	**0%**	**50%**	**100%**
Red	211.41	190.48	177.33
Green	**192.88**	**113.45**	**91.37**
Blue	167.7	117.64	101.33

(a)

Standard	**0%**	**50%**	**100%**
Red	211.41	172.43	154.37
Green	**192.88**	**99.64**	**75.37**
Blue	167.7	79.56	57.96

(b)

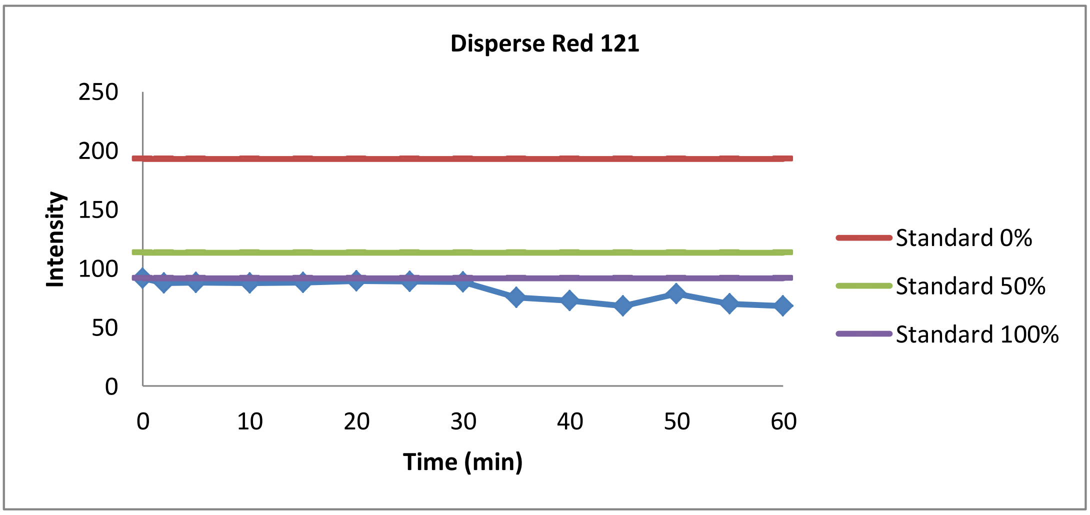

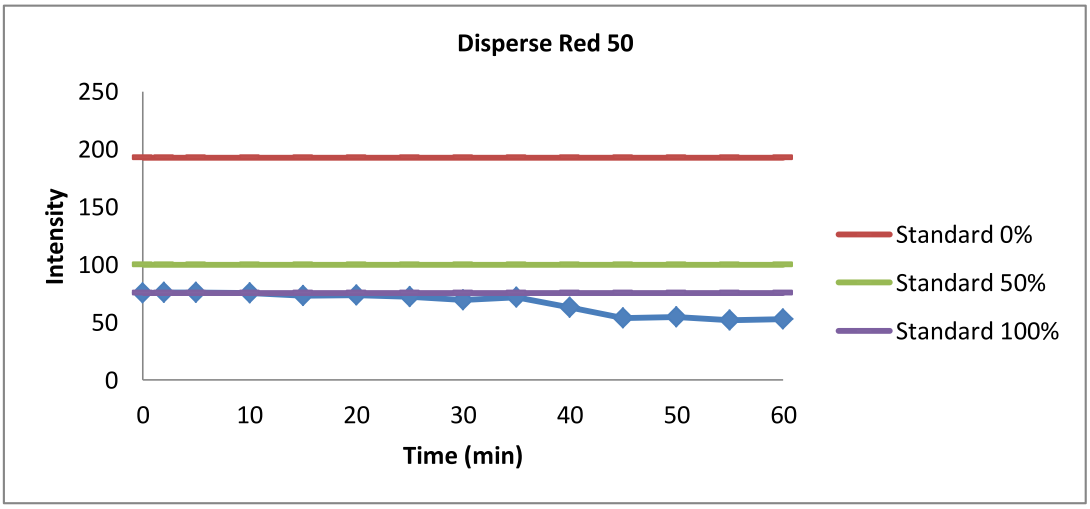

Figure 3.15 Effect TiO_2 photocatalysis on CI Disperse Red 121 and CI Disperse Red 50 after 60 minutes of UV irradiation

Table 3.10 Intensity data from Image J analysis, (a) CI Reactive Blue 19 and (b) CI Reactive Blue 4

Time	**Intensity**		
	Red	**Green**	**Blue**
2	49.57	57.24	93.71
5	54.5	60.98	87.76
10	54.27	59.3	83.88
15	56	58.85	79.22
20	58.68	59.13	77.21
25	61.5	61.36	78.39
30	64.35	62.76	77.58
35	68.95	65.71	79.22
40	69.12	65.2	75.66
45	75.89	69.92	79.07
50	80.48	73.36	83.9
55	82.17	74.12	84.05
60	90.99	79.59	84.56

Time	**Intensity**		
	Red	**Green**	**Blue**
2	84.68	95.7	120.51
5	87.54	97.19	115.69
10	88.71	97.85	115.79
15	89.63	96.77	110.22
20	93.61	99.61	111.93
25	95.77	99.12	109.2
30	98.84	100.76	109.43
35	96.2	98.19	106.15
40	100.05	100.46	105.72
45	94	93.91	98.62
50	98.73	98.07	101.99
55	100.89	99.3	101.99
60	107.14	103.81	105.92

Standard	**0%**	**50%**	**100%**
Red	**211.41**	**74.87**	**47.1**
Green	192.88	77.61	54.89
Blue	167.7	115.11	100.39

(a)

Standard	**0%**	**50%**	**100%**
Red	**211.41**	**99.52**	**84.68**
Green	192.88	107.78	97.69
Blue	167.7	131.62	127.37

(b)

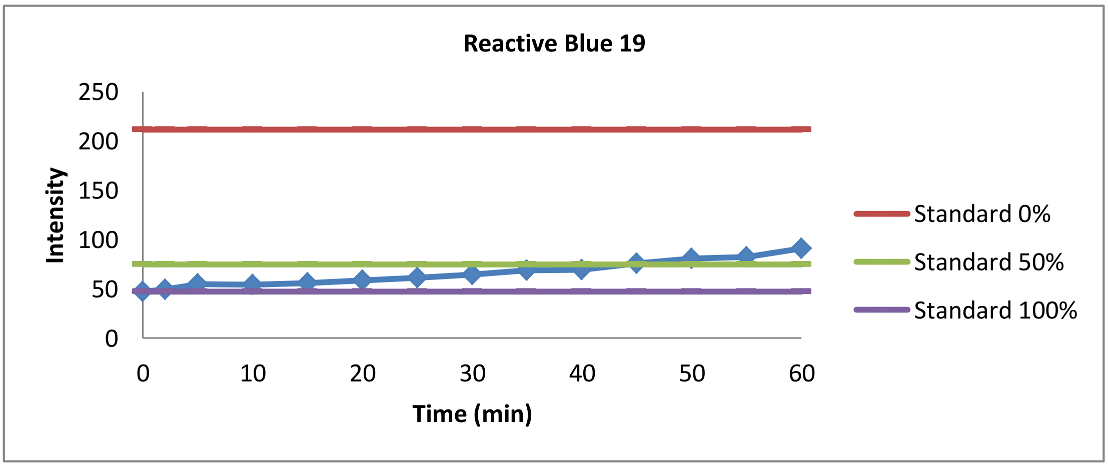

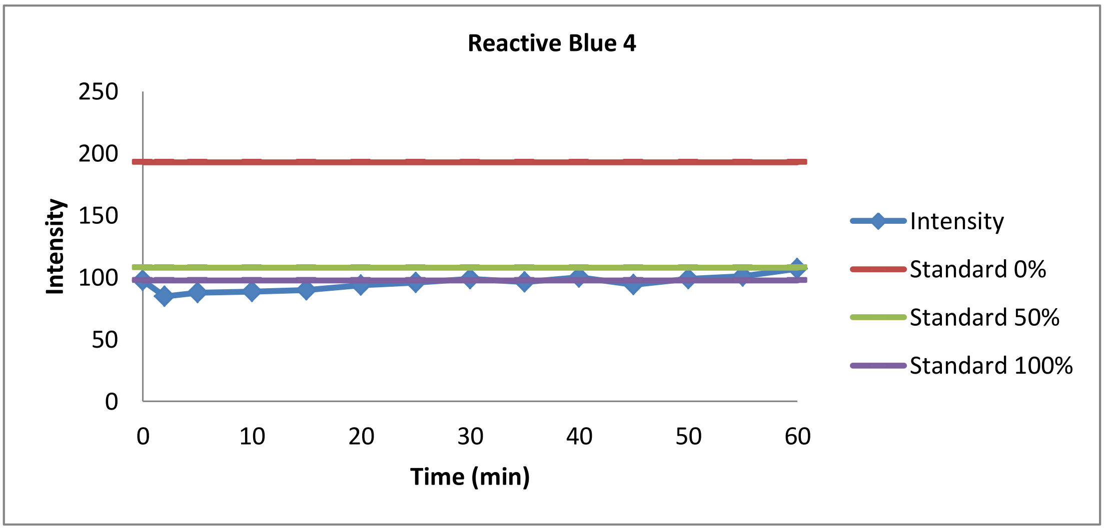

Figure 3.16 Effect TiO_2 photocatalysis on CI Reactive Blue 19 and CI Reactive Blue 4 after 60 minutes of UV irradiation

Table 3.11 Intensity data from Image J analysis, (a) CI Acid Blue 158 and (b) CI Reactive Yellow 44

Time	Intensity		
	Red	**Green**	**Blue**
2	37.49	53.65	80.4
5	43.22	56.93	82.89
10	47.15	59.85	83.4
15	52.06	63.09	89.08
20	52.07	63.45	88.39
25	51.56	62.21	82.57
30	56.57	66.38	89.05
35	58.45	68.05	90.7
40	62.21	68.94	88.09
45	63.2	71.95	94.24
50	64.46	72.79	94.41
55	62.23	69.72	90.73
60	60.28	66.36	88.86

Time	Intensity		
	Red	**Green**	**Blue**
2	197.81	155.45	32.08
5	193.1	144.33	33
10	186.56	137.09	31.73
15	177.04	125.47	29.05
20	181.96	130.44	32.46
25	181	129.48	35.43
30	182.23	130.48	37.53
35	175.28	124.39	36.69
40	184.63	133.49	41.67
45	181.75	128.83	40.62
50	182.9	130.77	43.06
55	183.6	131.78	45.01
60	182.9	131.93	45.61

Standard	**0%**	**50%**	**100%**
Red	**203.24**	**45.64**	**35.18**
Green	185.18	65.94	57.73
Blue	159.57	91.67	80.98

(a)

Standard	**0%**	**50%**	**100%**
Red	203.24	200.91	203.72
Green	185.18	170.57	166.16
Blue	**159.57**	**46.79**	**29.6**

(b)

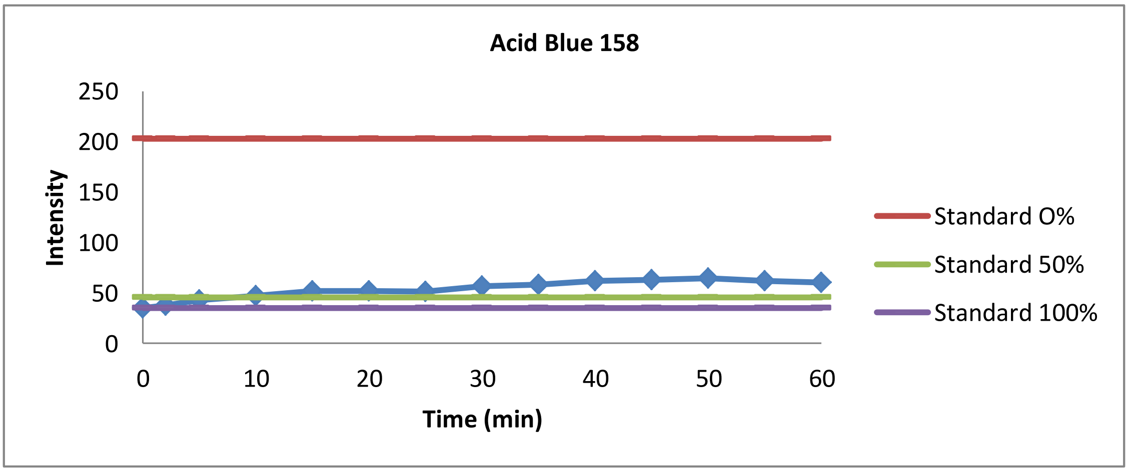

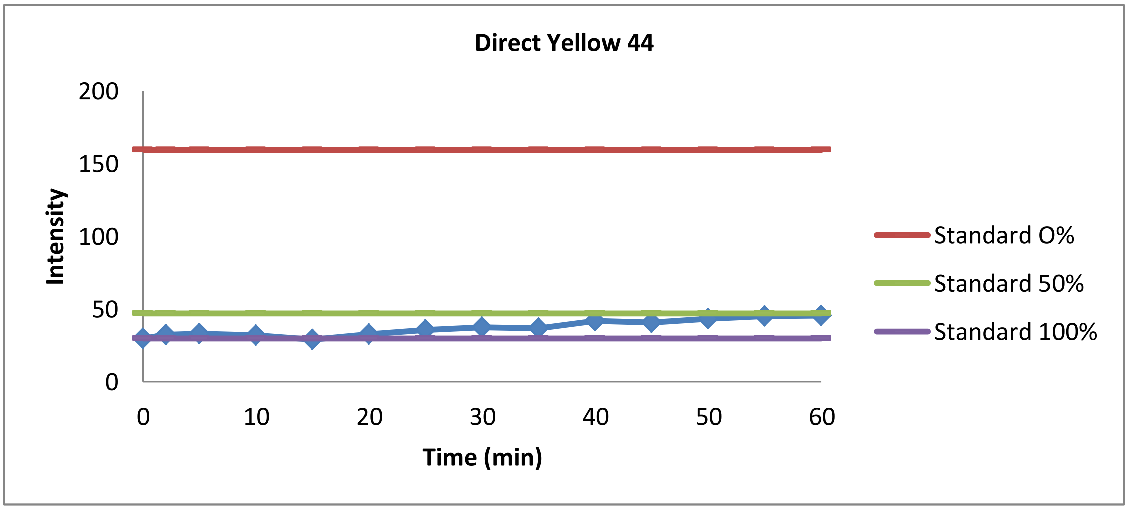

Figure 3.17 Effect TiO_2 photocatalysis on CI Acid Blue 158 and CI Direct Yellow 44 after 60 minutes of UV irradiation

Photocatalytic degradation of organic compounds occurs when TiO_2 + organic compound solution is irradiated with UV light (388 nm). This involves the excitation of electron in VB is excited into CB and results in the formation of an excited electron (e^-) and a positive hole (h^+) pair. This stage is referred as the semiconductor's 'photo-excitation' state.

The positive-hole of titanium dioxide breaks apart the water molecule to form hydrogen gas and hydroxyl radical. The negative-electron reacts with oxygen molecule to form super oxide anion. The resulting $^{\bullet}OH$ radical, being a very strong oxidizing agent (standard redox potential +2.8 V) can oxidize most of azo dyes to the mineral end-products. Substrates not reactive toward hydroxyl radicals are degraded employing TiO_2 photocatalysis with rates of decay highly influenced by the semiconductor valence band edge position.

Images taken during irradiation in five minute interval are presented in Appendix 1 – 10 and Appendix 11 – 12 represent images after filtration and centrifuge of the irradiated dye samples.

4. CONCLUSSION

Three methods of wastewater treatment used for the ten selected dyestuffs: classical way (coagulation), flocculation and photocatalysis. Classical way also used for the treatment of five simulated dyebaths (CI Acid Yellow 11, CI Direct Blue 106, CI Reactive Blue 4, CI Disperse Red 121 and CI Acid Blue 158).

All of the dyes were successfully treated by classical way (coagulation), with only slow settling volume when applied to simulated dyebaths. The azo dyes, CI Acid Yellow 11, CI Disperse Red 50, CI Direct Yellow 44 and CI Acid Red 213 showed 57 %, 57 %, 55 % and 54 % aggregate settling after one hour, and comparing to simulated dyebaths the settling volume of CI Acid Yellow 11 dropped from 57 to 49 %. The other standardised method (flocculation) proved successful only on disperse dyes.

The demonstration from the results that degradation or decolourisation by UV/TiO_2 photocatalysis was in used experiment much faster (50 % colour removed in 30 min) except on CI Acid Yellow 11 and the three disperse dyes (Yellow 42, Red 121 and Red 50). The resistance to photocatalytic decolourization by Acid Yellow 11 could be due to chemical composition of the dye.

On disperse dyes the resistance to decolourisation by UV/TiO_2 could be as a result of auxiliary (dispersing) agents on the surface of dye particle. It is possible that on irradiation of titanium oxide P25 Degussa by UV, the hydroxy radicals generated first reacted with these dispersing agents resulting in a darker colour of system by sedimentation process. During treatment the disperse dye sample were assessed visually, and the sediments of dark particles observed as from the first 5 minute of treatment, and this could be an advantage in separating the dye particles from water and also to degrade dispersing agent polymers which known for their polymeric nature and the presence of stable benzenoid rings, most lignosulphonate and formaldehydenaphthalenesulphonate dispersing agents are only bioeliminated to about 30% during textile effluent treatment.

5. REFERENCES:

[1]. Marco Paulo Gomes de Sousa Lucas. October 2009. Application of Advanced Oxidation Processes to Wastewater Treatment. Retrieved 26.09.2010. repositorio.utad.pt/bitstream/10348/314/1/phd_mpgslucas.pdf

[2]. Bamfield P. (2001). Chromic Phenomena. The Technological Applications of Colour Chemistry. UK: The Royal Society of Chemistry.ISBN 0-8404-474-4

[3]. Emission Scenario Document on Textile Finishing Industry. 24 June 2004. OECD. Series on Emission Scenario Documents. Retrieved 15.05.2010. www.oecd.org/document

[4]. Erkurt H.A. (2010). Biodegradation of Azo Dyes. The Handbook of Environmental Chemistry. Vol 9. Springer: New York. ISBN 978-3-642-11846-3

[5]. Shore J. (2002). Colourants and Auxiliaries. Organic Chemistry and Applications. No 2, Vol 1. Society of Dyers and Colourists.

[6]. Broadbent A.D. (2001). Basic Principles of Textile Colouration. Society of Dyers and Colourists. ISBN 0-901956-76-7

[7].Coagulation and Flocculation in Water and Wastewater Treatment. Retrieved 15.02.2011. www.iwawaterwiki.org.

[8]. Ingamells W. 1993. Colour for Textiles. Society of Dyers and Colourists. ISBN 0 901956 562.

[9]. El, Goresy; Chen, M; Dubrovinsky, L; Gillet, P; Graup, G, (2001). An ultradense polymorph of rutile with seven coordinated titanium from the Ries crater. Science 293 (5534): 1467 – 70

[10]. Emsley, J. 2001. Nature’s Building Blocks: A-Z Guide to the Elements. Oxford: Oxford University Press. Pp. 451 – 53. ISBN 0-19-850341-5

[11]. In situ doped titanium dioxide nanotubes come out on top. Retrieved 03.06. 2011. http://nanotechweb.org

[12] Ohno T, Sarukawa K, Tokieda K, and Matsumura M. 2001. Morphology of a TiO_2 Photocatalyst (Degussa, P-25) Consisting of Anatase and Rutile Crystalline Phases. Journal of Catalysis 203, 82-86

[13] Bickley, R. I., Gonzalez-Carreno, T., Lees, J. S., Palmisano, L., and Tilley, R. D., J. 1991. Solid State Chem. 92, 178

[14] Datye, A. K., Riegel, G., Bolton, J. R., Huang, M., and Prairie, M. R., J. 1995. Solid State Chem. 115, 236

[15] Tyner K. M, Mokovich A. M, Godar D. E, Doub W. H, Sadrieh N. The state of nano-sized titanium dioxide (TiO_2) may affect sunscreen performance. 2011. International Journal of Cosmetic Science. 1-15

[16] 17^{th} International Conference on Photochemical Conversion and Storage of Solar Energy. 2008. Sydney Convention and Exhibition Centre, Sydney, Australia. Retrieved 08.03.2011. www.chse.unsw.edu.au

[17] Ioannis K. Konstantinou, Triantafyllos A. Albanis. 2004. TiO2-assisted photocatalytic degradation of azo dyes in aqueous solution. Applied Catalysis B: Environmental 49, 1–14

[18] Ju-Young Park, Changhoon Lee, Kwang-Woo Jung, and Dongwoon Jung. 2009. Structure Related Photocatalytic Properties of TiO2. Korean Chem. Soc., Vol. 30

[19] Kaneko, M. Okura, I. 2002.Photocatalysis (Science and Technology). Kodasha Ltd. Tokyo, ISBN 4-06-210615-9

[20] Fujishma A. Zhang X. Donald A. 2008.TiO2 photocatalysis and related surface phenomena, Surface Science reports 63, 515 – 582

[21] Teichner, S, J. 2008. The origins of photocatalysis. J Porous Mater 15, 311–314

[22] Dilek Gümüş & Feryal Akbal. 2011. Photocatalytic Degradation of Textile Dye and Wastewater. Water Air Soil Pollut 216:117–124

[23] Tanaka K, Padermpole K and Hisanaga T. 1999. Photocatalytic Degradation of Commercial Azo Dyes. National Institute of Materials and Chemical Research. Wat. Res. Vol. 34, No. 1, pp. 327±333

[24] Chih-Yu Chen. 2009. Photocatalytic Degradation of Azo Dye Reactive Orange 16 by TiO2. Water Air Soil Pollut 202:335–342

[25] Advanced Photocatalyst Manufacture. Visible Light Nano Photocatalysis. Retireved 25.03.2011.www.tipe.com.cn

[26] ATLAS UV + Photo-Catalysis Technology -Atlas Industrial Group Cop. Retrieved 15.02.2011. http://www.atlasgroupe.com

[27] Hashimoto K, Irie H, Fujishma A. 2005. TiO2 Photocatalysis: A Historical Overview and Future Prospects. . Japanese Journal of Applied Physics. Vol. 44, No. 12, 8269–8285

[28] D.R. Kennedy, M. Ritchie, J. Mackenzie, Trans. Faraday Soc. 54 (1958)

[29] I.S. McLintock, M. Ritchie, Trans. Faraday Soc. 61 (1965) 1007_1016

[30] J. Peral, D.F. Ollis, J. Catal. 136 (1992) 554_565.

[31] L.A. Phillips, G.B. Raupp, J. Molec. Catal. 77 (1992) 297_311.

[32] G.B. Raupp, C.T. Junio, Appl. Surf. Sci. 72 (1993) 321_327.

[33] T.N. Obee, R.T. Brown, Environ. Sci. Technol. 29 (1995) 1223_1231.

[35] Coagulation & Flocculation for Raw Water. Retrieved 03.05.2011. www.nalco.com

[35] Water Treatment. Coagulation and Flocculation. Retrieved 29.04.2011. ocw.tudelft.nl

6. APPENDIX

Appendix A 1

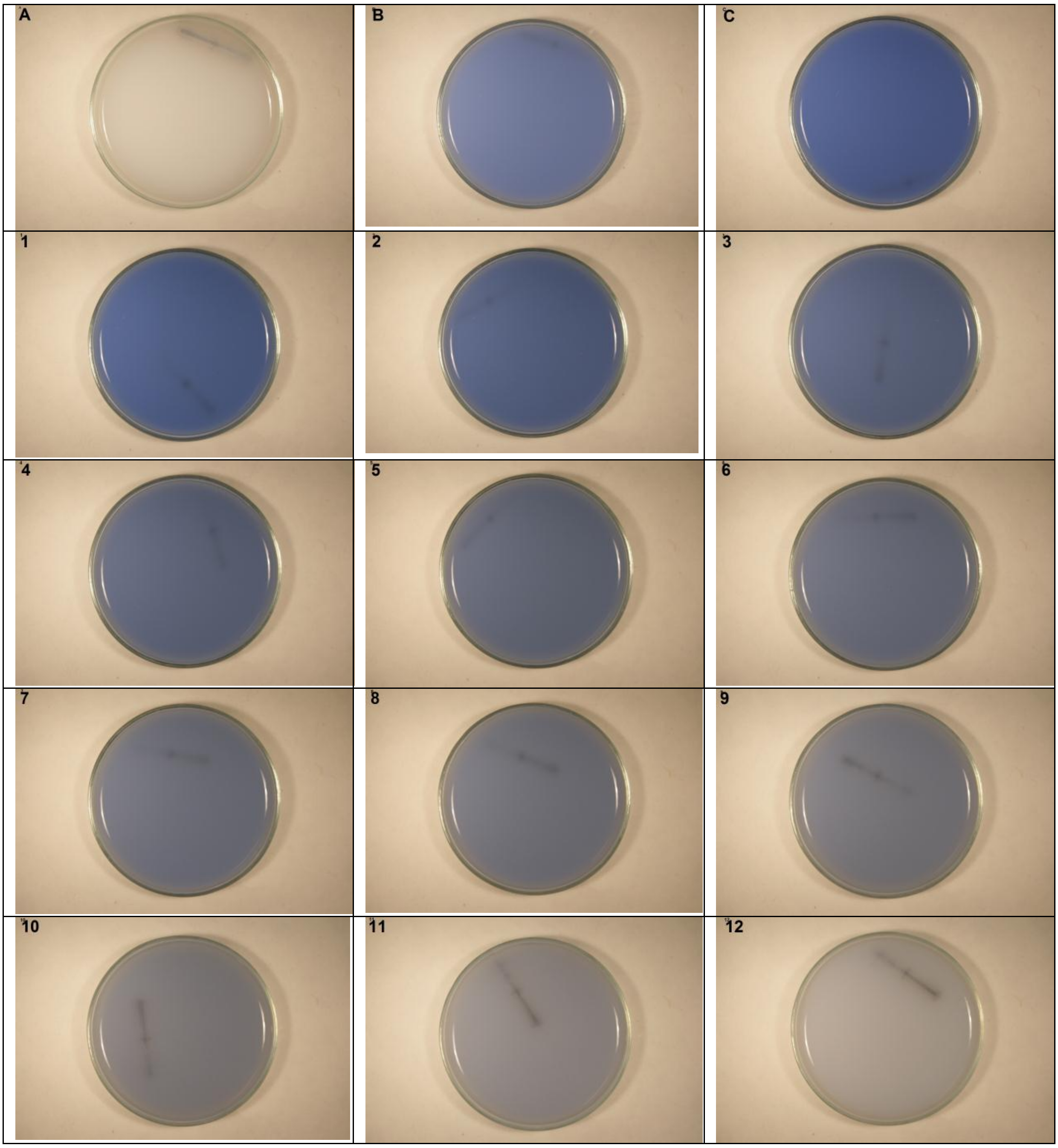

Images of CI Direct Blue 106 taken in 5 minute intervals for 60 minutes.

A = Standard 0%, B = Standard 50% and C = Standard 100%

Appendix A 2

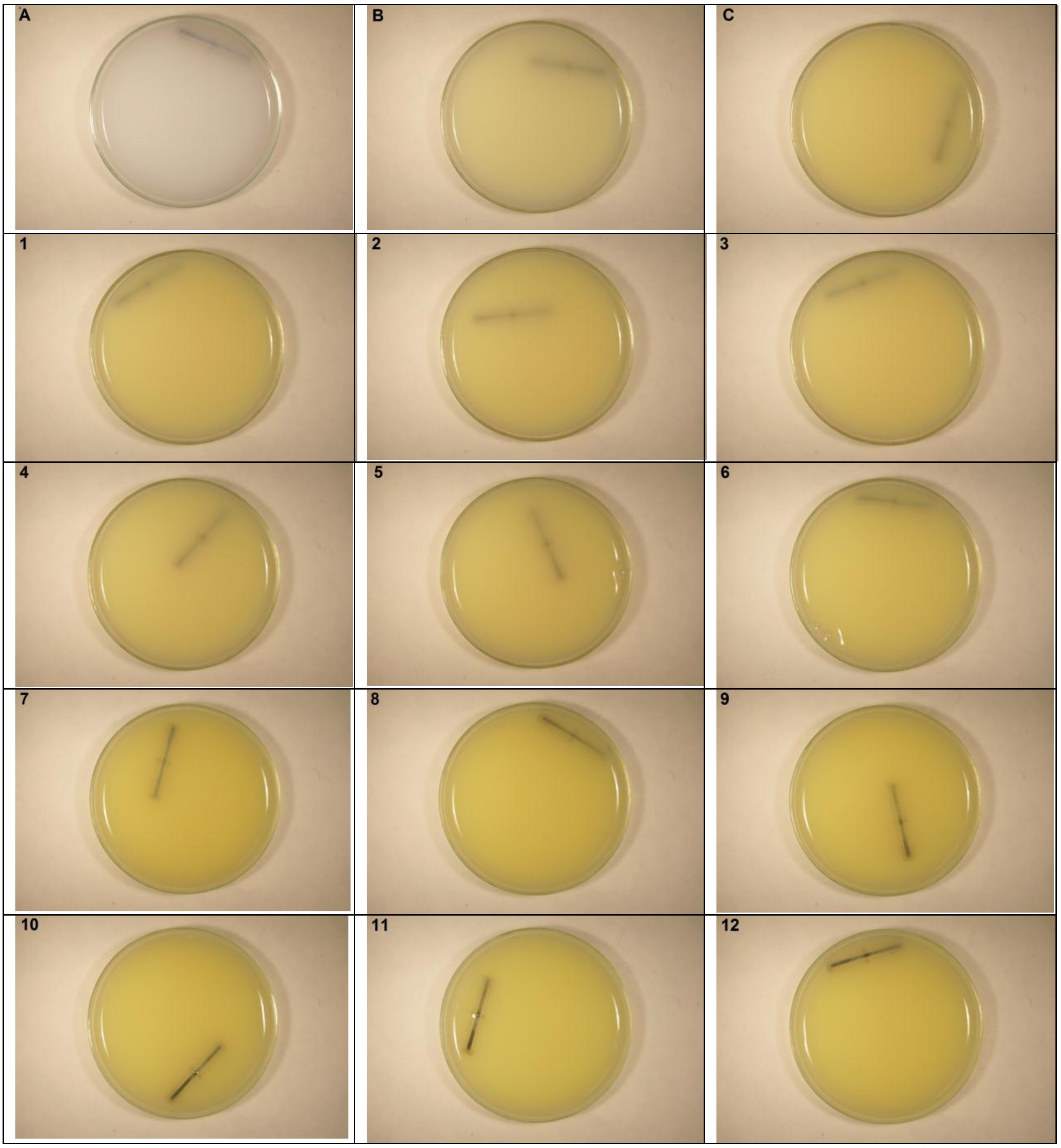

Images of CI Direct Blue 106 taken in 5 minute intervals for 60 minutes.

A = Standard 0%, B = Standard 50% and C = Standard 100%

Appendix A 3

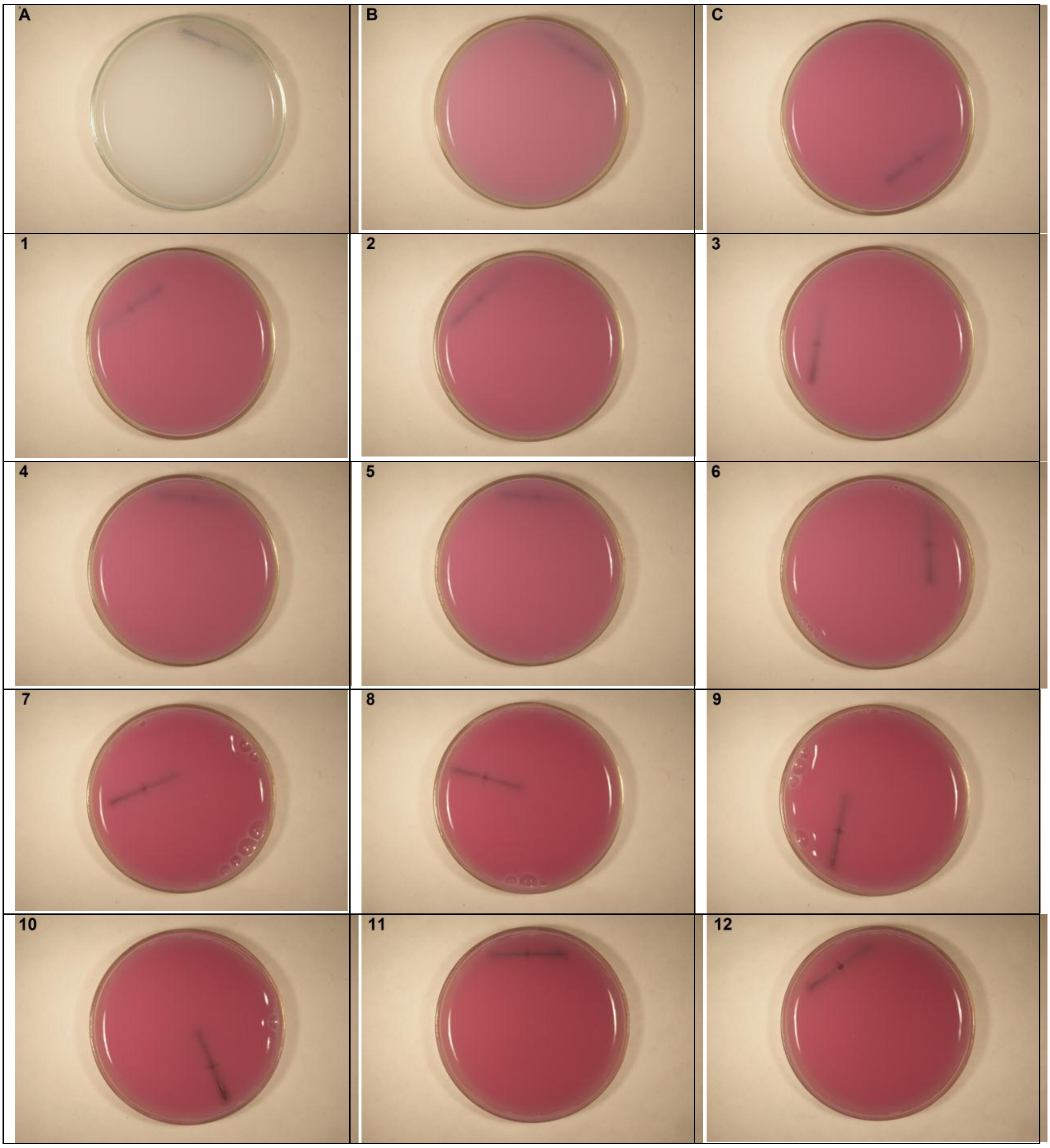

Images of CI Direct Blue 106 taken in 5 minute intervals for 60 minutes.

A = Standard 0%, B = Standard 50% and C = Standard 100%

Appendix A 4

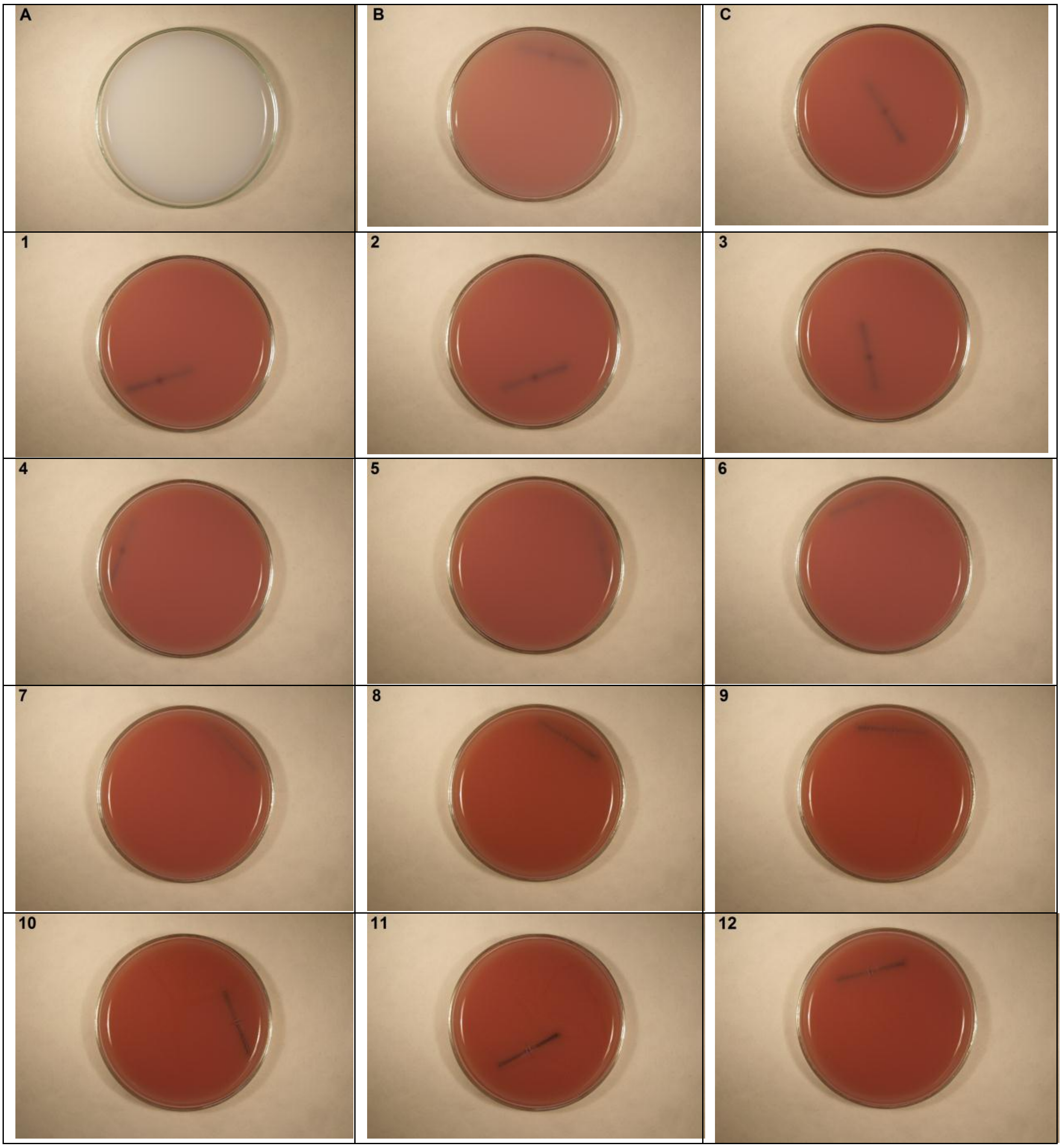

Images of CI Direct Blue 106 taken in 5 minute intervals for 60 minutes.

A = Standard 0%, B = Standard 50% and C = Standard 100%

Appendix A 5

Images of CI Direct Blue 106 taken in 5 minute intervals for 60 minutes.

A = Standard 0%, B = Standard 50% and C = Standard 100%

Appendix A 6

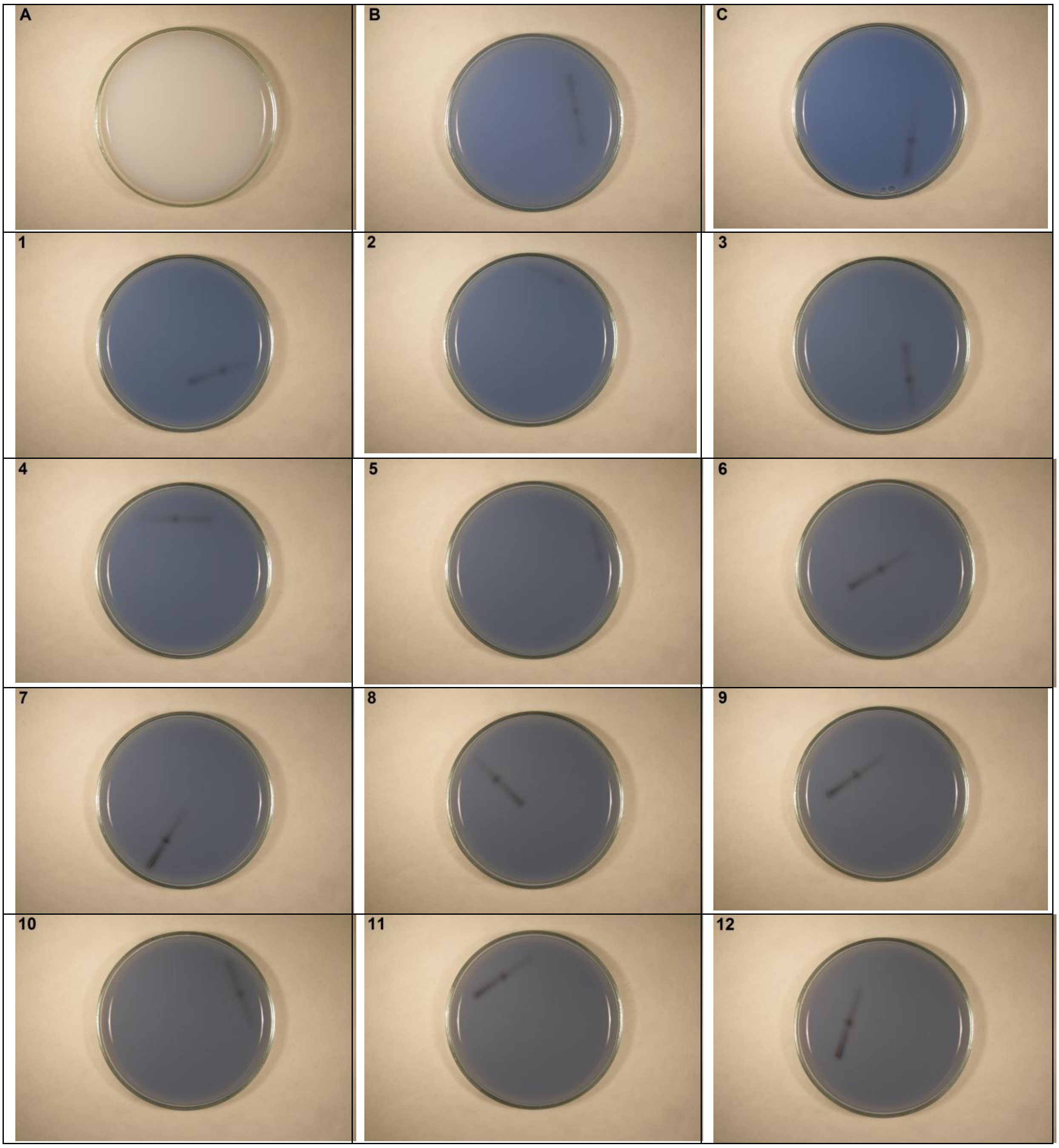

Images of CI Direct Blue 106 taken in 5 minute intervals for 60 minutes.

A = Standard 0%, B = Standard 50% and C = Standard 100%

Appendix A 7

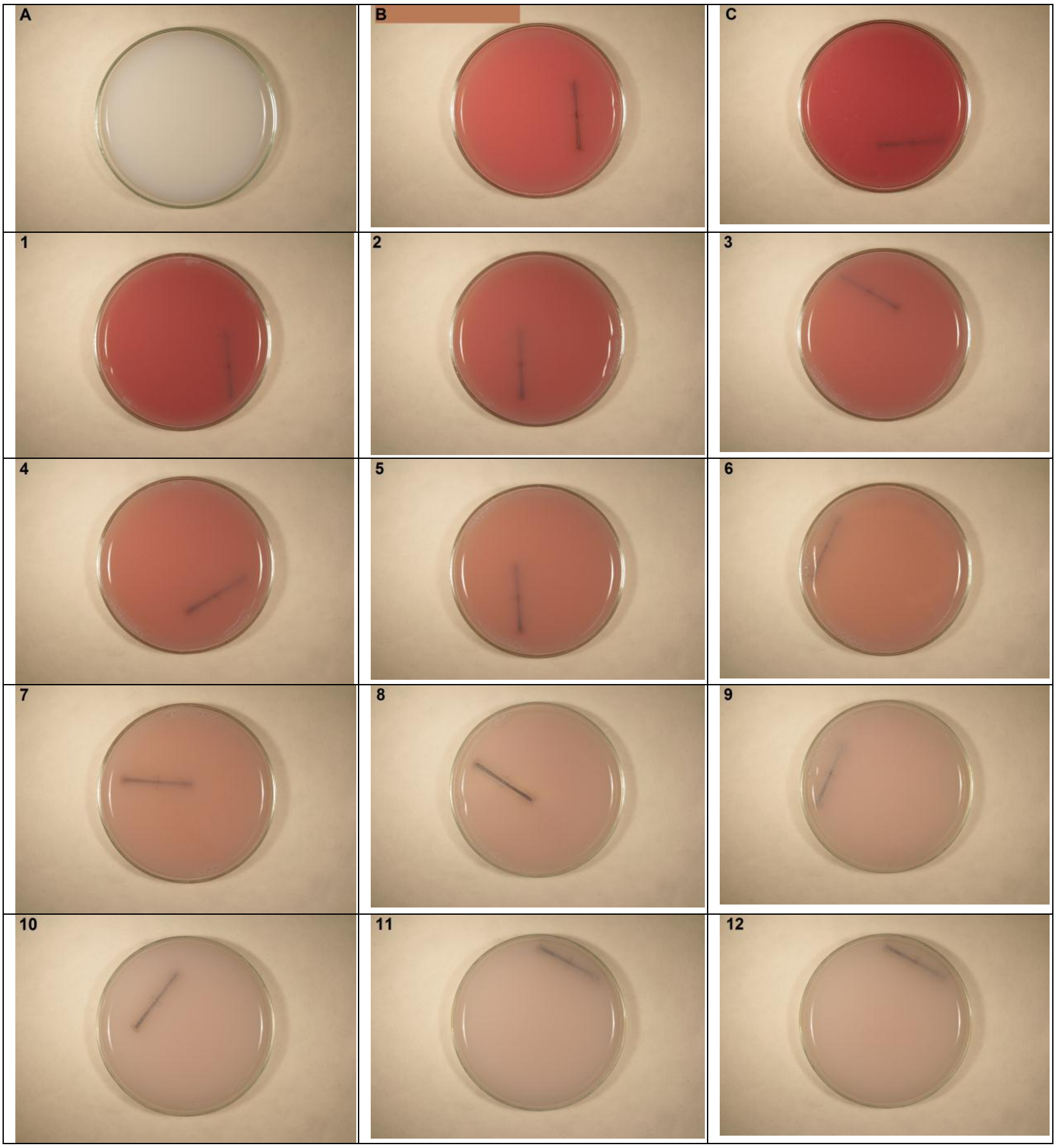

Images of CI Direct Blue 106 taken in 5 minute intervals for 60 minutes.

A = Standard 0%, B = Standard 50% and C = Standard 100%

Appendix A 8

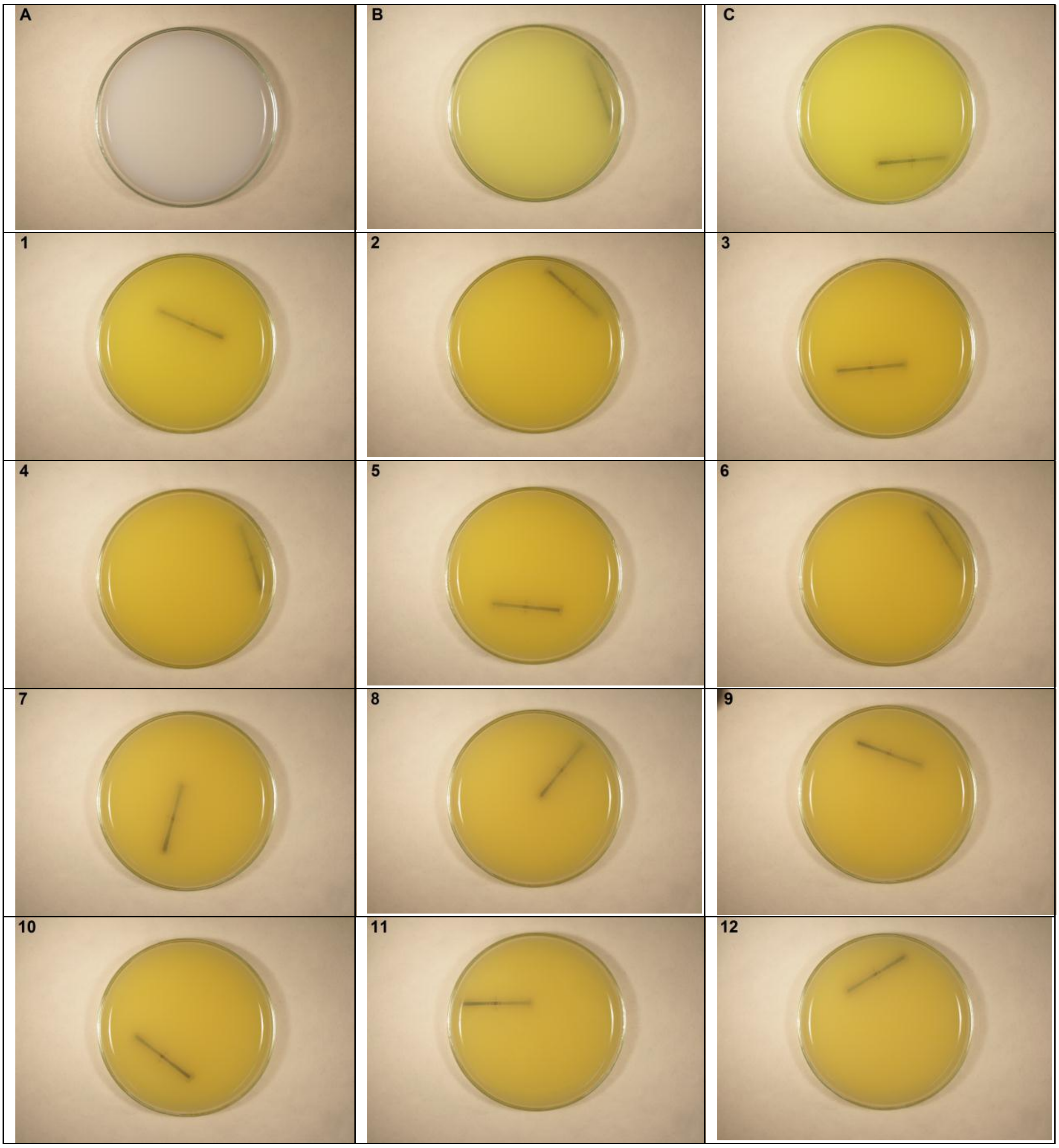

Images of CI Direct Blue 106 taken in 5 minute intervals for 60 minutes.

A = Standard 0%, B = Standard 50% and C = Standard 100%

Appendix A 9

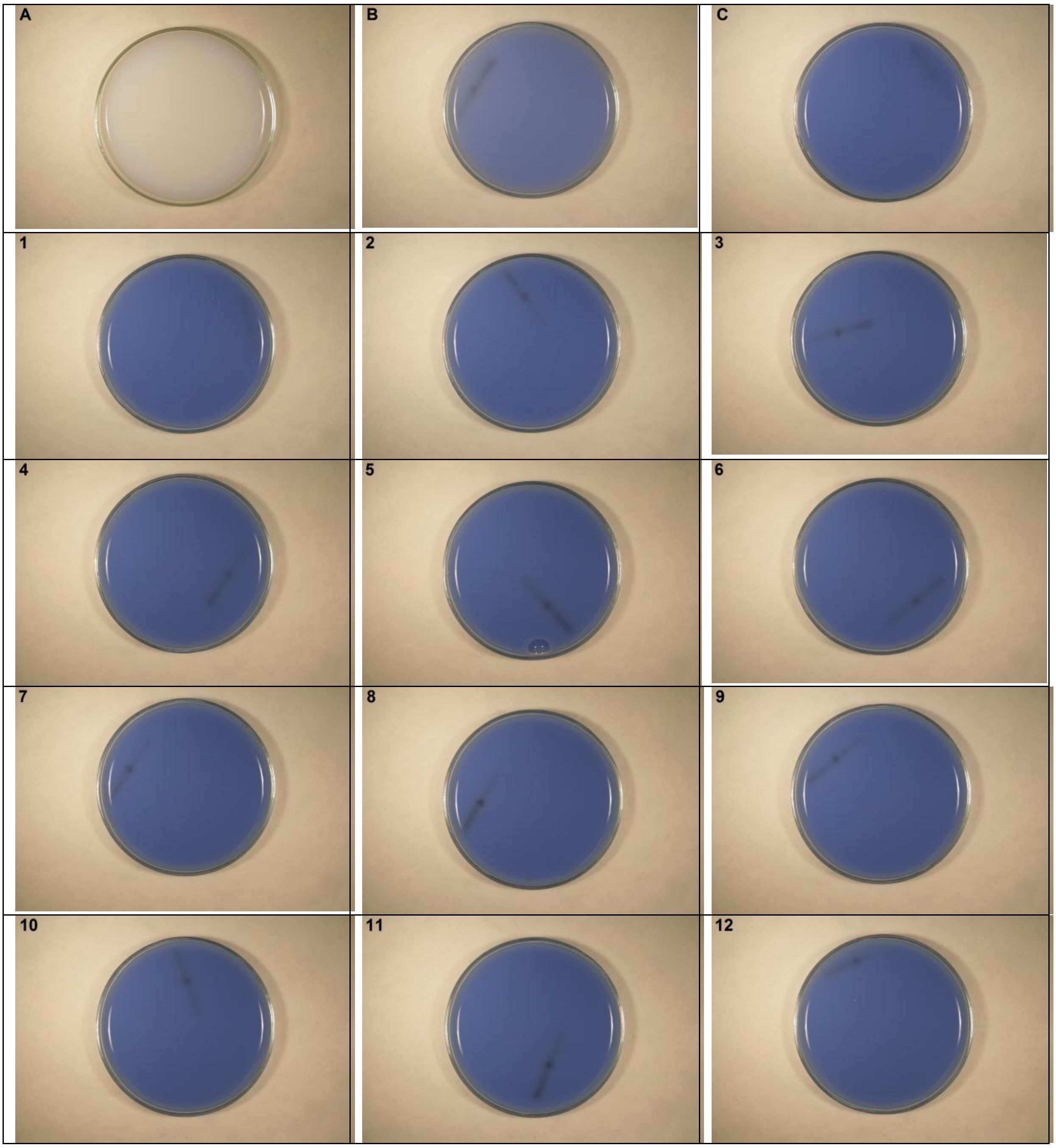

Images of CI Direct Blue 106 taken in 5 minute intervals for 60 minutes.

A = Standard 0%, B = Standard 50% and C = Standard 100%

Appendix A 10

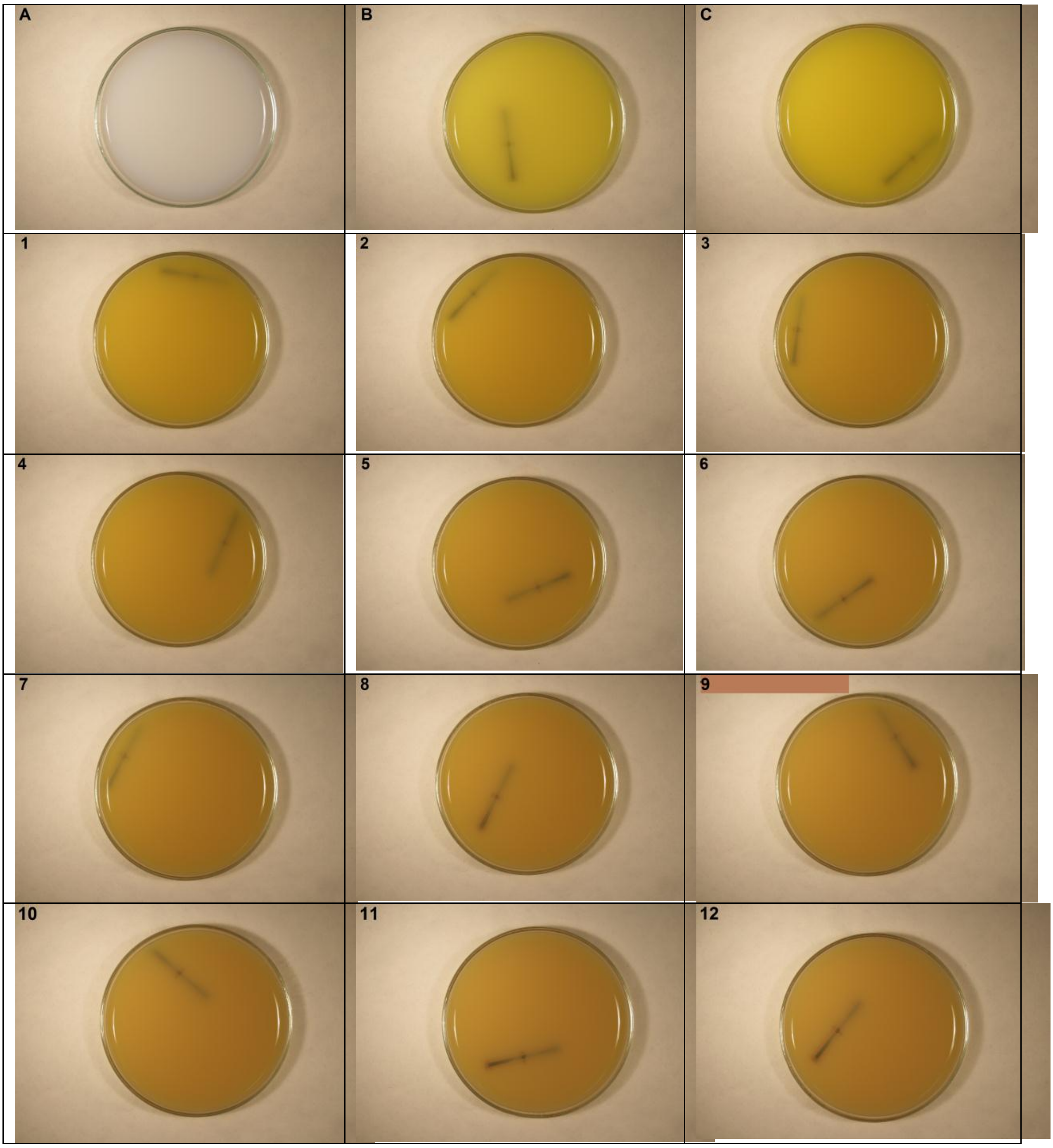

Images of CI Direct Direct Yellow 44 taken in 5 minute intervals for 60 minutes.

A = Standard 0%, B = Standard 50% and C = Standard 100%

Appendix A 11

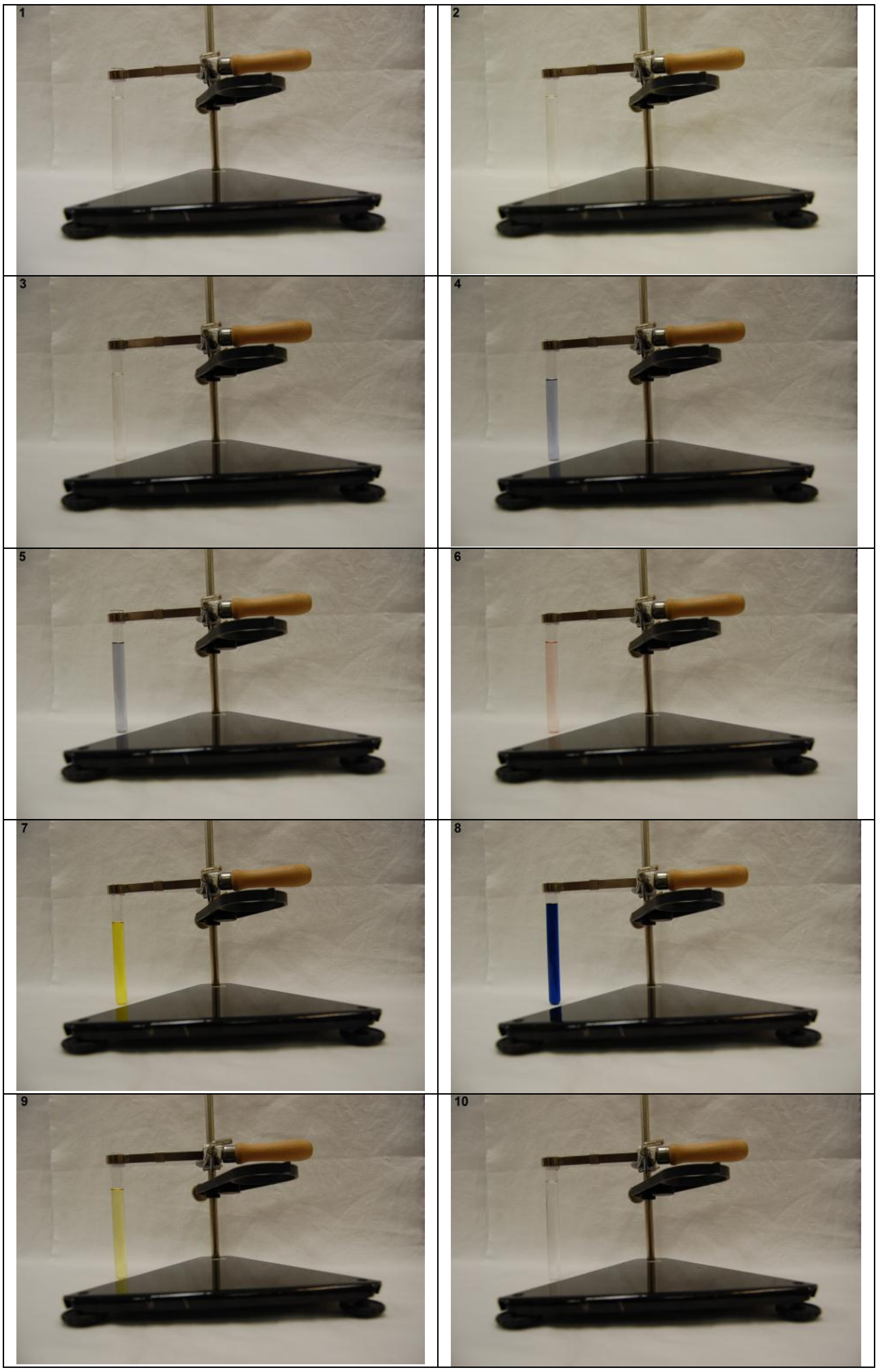

Images of UV/TiO2 treated samples after centrifuge.

1= Disperse Yellow 42, 2 = Disperse Red 121, 3 = Disperse Red 50, 4 = Direct Yellow 44, Reactive Blue 19, Reactive Blue 4, 6= Acid Red 213, 7 = Acid Yellow 11; 8 = Acid Blue 158, 9 = Direct Yellow 44, 10 = Direct Blue 106 Yellow 42.

Appendix A 12

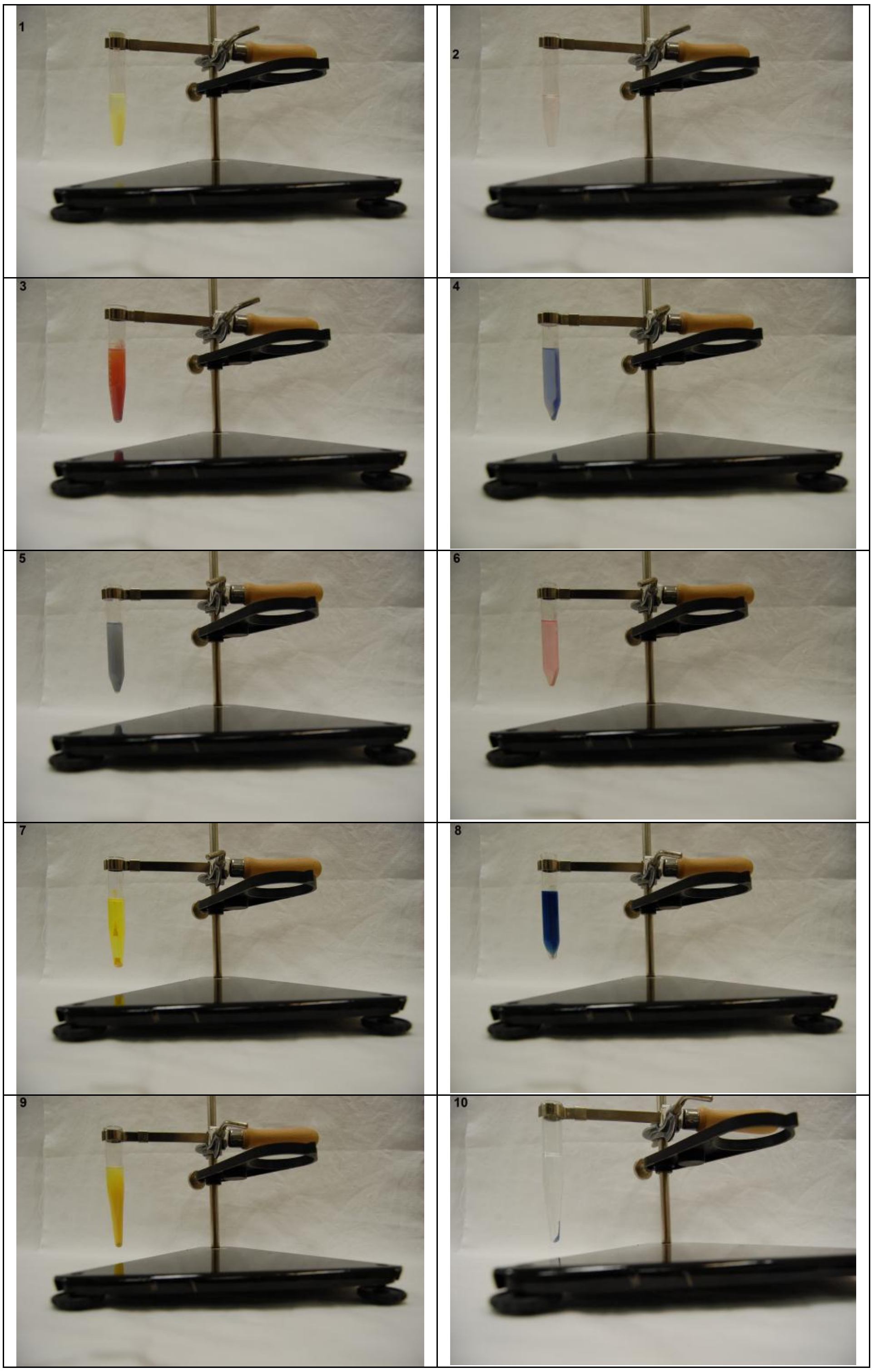

Images of UV/TiO2 treated samples after centrifuge.

1= Disperse Yellow 42, 2 = Disperse Red 121, 3 = Disperse Red 50, 4 = Direct Yellow 44, Reactive Blue 19, Reactive Blue 4, 6= Acid Red 213, 7 = Acid Yellow 11; 8 = Acid Blue 158, 9 = Direct Yellow 44, 10 = Direct Blue 106 Yellow 42.